

Semiparametric semi-supervised learning for general targets under distribution shift and decaying overlap

Lorenzo Testa^{1,2}, Qi Xu¹, Jing Lei¹, and Kathryn Roeder^{1,3}

¹Department of Statistics & Data Science, Carnegie Mellon University

²L'EMbeDS, Sant'Anna School of Advanced Studies

³Department of Computational Biology, Carnegie Mellon University

{ltesta,qixu,jinglei,roeder}@andrew.cmu.edu

March 3, 2026

Abstract

In modern scientific applications, large volumes of covariate data are readily available, while outcome labels are costly, sparse, and often subject to distribution shift. This asymmetry has spurred interest in semi-supervised (SS) learning, but most existing approaches rely on strong assumptions – such as missing completely at random (MCAR) labeling or strict positivity – that put substantial limitations on their practical usefulness. In this work, we introduce a general semiparametric framework for estimation and inference in SS settings where labels are missing at random (MAR) and the overlap may vanish as sample size increases. Our framework, that we label D^2S^3 , accommodates a wide range of smooth statistical targets – including means, linear regression coefficients, quantiles, and causal effects – and remains valid under high-dimensional nuisance estimation and distributional shift between labeled and unlabeled samples. We extend the theoretical guarantees of augmented inverse probability weighting estimators to preserve double robustness and asymptotically normality under this challenging D^2S^3 regime. A key insight is that classical root- n convergence fails under vanishing overlap; we instead provide corrected asymptotic rates that capture the impact of the decay in overlap. We validate our theory through simulations and demonstrate practical utility in real-world applications on the internet of things and public health where labeled data are scarce.

1 Introduction

In contemporary scientific applications, as highlighted by the success of *prediction-powered inference* (Angelopoulos et al., 2023a), semi-supervised (SS) learning has emerged as a powerful and increasingly essential paradigm, particularly in contexts where labeled data are expensive, difficult, or ethically challenging to obtain. These situations are ubiquitous in scientific domains such as biomedical research (e.g., large biobanks with partial annotations), public policy analysis (e.g., outcomes available only for selected sub-populations) and digital platforms (e.g., engagement or intervention data available only for active users). In these settings, researchers typically have access to a large volume of unlabeled covariate information, whereas labeled observations – i.e., data points with observed outcomes of interest – remain sparse.

A fundamental and often overlooked consequence of this asymmetry is the inherent *violation* of the *positivity* or *overlap* condition. As the amount of unlabeled data grows much faster than the number of labeled samples, it becomes increasingly likely that certain covariate regions are labeled with vanishing probability. Formally, the labeling propensity, defined as the conditional probability of observing the outcome given the covariate, may approach zero on non-negligible portions of the covariate space, violating the standard assumption that the labeling propensity is bounded away from zero almost surely. This phenomenon, known as *overlap decay*, is not merely a technicality, but a structural feature of semi-

supervised learning. It affects estimation and inference, and renders many traditional estimators unstable. Crucially, this distinguishes the semi-supervised setting from standard missing data problems, where the labeling mechanism is always assumed to satisfy overlap conditions (Tsiatis, 2006). In SS learning, by contrast, decaying overlap is the norm, and asymptotic theory must be adapted accordingly.

Moreover, much of the existing work in semi-supervised learning (Angelopoulos et al., 2023a; Xu et al., 2025) has been developed under the assumption that labels are *missing completely at random* (MCAR), where the probability of observing a label is independent of both covariates and outcomes. Although analytically convenient, this assumption is rarely plausible in practice, especially in observational studies. In real-world applications where randomized design cannot be implemented, the labeling process is almost always influenced by observable characteristics, such as patient demographics, policy priorities, or platform usage patterns, making the MCAR assumption often inappropriate. A more realistic framework is the *missing at random* (MAR) setting, where the labeling probability depends on the covariates, but is conditionally independent of the unobserved outcome. The MAR assumption, also known as *ignorability* condition or *selection bias*, allows systematic *distribution shift* patterns in the labeling mechanism, while still permitting identifiability of the outcome distribution from observed data.

Under this *decaying distribution shift semi-supervised* (D^2S^3) framework, naive applications of existing semi-supervised or missing data methods can yield biased or inefficient estimates, or even fail to be well defined. In this paper, we propose a general semiparametric framework for estimation and inference in semi-supervised settings under distribution shift and decaying overlap. Our framework covers a wide range of statistical inference targets – including means, causal effects, quantiles, and smooth functionals of the data-generating process – and offers principled strategies for estimation even when the probability of observing a label vanishes in large regions of the covariate space. Crucially, our theory allows for distributional shift between the labeled and unlabeled samples, meaning that the covariate distributions can be different, so long as appropriate reweighting can be performed with accurate nuisance parameter estimation.

We build on semiparametric efficiency theory to derive influence functions for *general* targets in the D^2S^3 setting, and characterize augmented inverse probability weighting (AIPW) estimators that are doubly robust, as they remain consistent and asymptotically normal even if one of the two nuisance components (labeling or projection) is misspecified. Moreover, we show that asymptotic normality remains attainable – though at a slower rate – provided that the decay in labeling probability is appropriately controlled. To our knowledge, this is the first investigation of the theoretical guarantees of augmented inverse probability weighting estimators for general parameters of interest under the D^2S^3 setting. A detailed comparison of our results with existing literature is provided in Section 1.1.

1.1 Related work

Our work, lying at the intersection of several branches of scholarship, combines the virtues of multiple literatures into a unified inferential framework for semi-supervised learning under distribution shift and decaying overlap.

“Pure” semi-supervised learning. SS learning has traditionally focused on settings in which the labeled data are assumed to be missing completely at random (MCAR) – see Chapelle et al. (2009); Zhu (2005) for a review. Most existing work in this area focuses on estimation methods tailored to specific problems, such as mean estimation (Zhang et al., 2019; Zhang and Bradic, 2022), quantile estimation (Chakraborty et al., 2022), and linear regression (Azriel et al., 2022; Cai and Guo, 2020). Notable exceptions are Song et al. (2024), which studies general M-estimation problems, and Xu et al. (2025), which encompasses all parameters satisfying some form of functional smoothness. However, the MCAR assumption is increasingly recognized as unrealistic in many scientific applications, limiting the practical utility of such techniques in the presence of distribution shift.

Prediction-powered inference. A recent line of work addressing semi-supervised learning under MCAR is the *prediction-powered inference* (PPI) framework. PPI integrates machine learning predictions into formal statistical procedures, using both labeled and unlabeled data to improve estimation efficiency

while maintaining valid inference, resembling the approach proposed by [Chen and Chen \(2000\)](#). Since the seminal work of [Angelopoulos et al. \(2023a\)](#), several extensions have expanded its scope. [Angelopoulos et al. \(2023b\)](#) and [Miao et al. \(2023\)](#) propose weighting strategies that ensure the PPI estimator performs at least as well as estimators relying solely on labeled data. [Zrnic and Candès \(2024\)](#) further develops the framework by introducing a cross-validation-based approach to learn the predictive model directly from the labeled sample. [Kluger et al. \(2025\)](#) generalizes PPI beyond M-estimation tasks and to MAR settings, assuming propensity scores are known by design. [Ji et al. \(2025\)](#) links PPI to surrogate outcome models in a MCAR setting. See [Carlson and Dell \(2025\)](#) for a summary of additional PPI extensions.

D²S³ setting. Classical results in semiparametric theory offer general principles for constructing doubly robust estimators in settings where outcomes are missing at random ([Tsiatis, 2006](#)). These estimators combine outcome projection models and propensity score models – estimated either from the labeled sample alone or by incorporating information from both labeled and unlabeled data – to yield consistent estimators of population-level parameters. However, most existing work assumes strong overlap. On the other hand, the literature on limited overlap and positivity violations has largely emerged from the causal inference community, where imbalance in treatment assignment and high-dimensional covariates pose analogous challenges ([Crump et al., 2009](#); [D’Amour et al., 2021](#); [Khan and Tamer, 2010](#); [Rothe, 2017](#); [Yang and Ding, 2018](#)). Proposed solutions include trimming low-overlap regions, covariate balancing, and targeted reweighting schemes that stabilize estimation by controlling variance in sparse areas. Nevertheless, these methods typically assume that the propensity score can approach zero only in some specific regions of the support of the covariates X and does not depend on the sample size. As such, they are ill-equipped to handle settings where the labeling probability vanishes uniformly across the covariate space as the total sample size grows. A notable exception is the recent work of [Zhang et al. \(2023b\)](#), who develop a doubly robust estimator for the outcome mean in a semi-supervised MAR setting with decaying overlap.

Semiparametric statistics and missing data. From a technical standpoint, our work lies in the furrow of semiparametric statistics, which focuses on estimation in the presence of high-dimensional nuisance parameters. The missing data literature provides tools such as inverse probability weighting, augmented IPW, and targeted maximum likelihood estimation, many of which naturally extend to SS learning with MAR labeling. Foundational results on influence functions, tangent spaces, and semiparametric efficiency bounds – developed by [Bickel et al. \(1993\)](#); [Tsiatis \(2006\)](#); [Van der Vaart \(2000\)](#) – serve as the theoretical backbone of modern SS learning inference. However, most of these frameworks assume strict positivity. As a result, applying semiparametric tools in semi-supervised learning with shrinking labeling fractions and decaying overlap requires substantial modifications to asymptotic analysis.

1.2 Our contributions

We propose a general framework for identification, estimation, and inference of arbitrary target parameters in the semi-supervised setting with missing at random labeling and decaying overlap. Our work builds on semiparametric theory, but departs significantly from classical setups by relaxing the positivity assumption and allowing the labeling probability to vanish uniformly as the sample size increases. Our main contributions are as follows:

- **General-purpose inference under decaying overlap.** We develop a flexible and model-agnostic D²S³ framework to accommodate estimation and inference of general target parameters under MAR labeling and decaying overlap. Our approach accommodates arbitrary functionals – such as means, causal effects, or linear regression coefficients – and handles distribution shifts without relying on parametric or Donsker-type assumptions about the projection functions or the missingness mechanism.
- **Nonstandard asymptotics and double robustness.** We extend the theoretical guarantees of augmented inverse probability weighting estimators to the D²S³ framework, showing that they preserve double robustness and asymptotically normality. Importantly, the central limit theorem we prove exhibits a non-standard dependence on the sample size that captures the effect of overlap

Scholarship	MAR	Decaying overlap	General target
Tsiatis (2006)	✓	✗	✓
Zhang et al. (2023b)	✓	✓	✗
PPI (Angelopoulos et al., 2023a)	✗	✗	✓
Xu et al. (2025)	✗	✗	✓
D ² S ³ (our proposal)	✓	✓	✓

Table 1: Framing our contribution

decay. This opens up the question of semiparametric efficiency in the D²S³ regime, in contrast to classical settings where the propensity score is fixed, i.e. does not decay as the sample size increases.

- **Prediction-powered inference under MAR.** As a side product of our theoretical and methodological development, we provide a natural extension of PPI to missing at random settings, greatly increasing its applicability in real-world scenarios.

Table 1 summarizes our contribution in relation to the existing literature, highlighting how our framework integrates MAR labeling, accommodates overlap decay, and supports general statistical targets.

1.3 Organization

This paper is organized as follows. Section 2 introduces the semi-supervised learning framework under MAR labeling with decaying overlap (D²S³), and formally defines the statistical estimation problem. In Section 3, we present a general strategy for building augmented inverse probability weighting estimators and characterize their asymptotic behavior under D²S³. Following Tsiatis (2006); Zhang et al. (2023b), we begin by analyzing the case where the propensity score is known by design, and then extend our results to the more realistic setting where the propensity score must be estimated from the data. Here, we also extend the *prediction-powered inference* framework proposed by Angelopoulos et al. (2023a) to the D²S³ setting. Section 4 applies our general theory to specific statistical functionals and assesses the empirical performance of AIPW in the D²S³ setting through simulation studies. In Section 5, we illustrate the practical value of our methodology using data from the BLE-RSSI study (Mohammadi et al., 2017), where we estimate the spatial position of a device based on signal strength measurements captured by remote sensors, and the NHEFS study (Ertefaie et al., 2023; Hernán and Robins, 2010), where we estimate the change in weight and smoking intensity in the population using only labeled data from alcohol abstainers. Concluding remarks and potential directions for future research are discussed in Section 6. Additional theoretical results, simulation details, and a further application to the METABRIC study (Curtis et al., 2012; Pereira et al., 2016), where we revisit a question posed by Hsu and Lin (2023) and estimate the association between previously identified biomarkers (Cheng et al., 2021) and survival outcomes in patients with breast cancer, are provided in the Supplementary Material. All code for reproducing our analysis is available at https://github.com/testalorenzo/decMAR_inf.

2 Problem setup

We assume that we observe a *small* collection of n independent and identically distributed *labeled* samples $\{\mathcal{D}_i^L = (X_i, Y_i)\}_{i=1}^n$, where $X_i \in \mathbb{R}^p$ is a p -dimensional vector of covariates and $Y_i \in \mathbb{R}^k$ is a k -dimensional outcome. We let $\mathcal{D}^L = (X, Y)$ denote an independent copy of $\mathcal{D}_i^L = (X_i, Y_i)$. We also assume to have access to a further *large* collection of N *unlabeled* data samples $\{\mathcal{D}_i^U = (X_i)\}_{i=1}^N$. As before, we let $\mathcal{D}^U = (X)$ denote an independent copy of $\mathcal{D}_i^U = (X_i)$. Following traditional nomenclature from semiparametric statistics literature, we recast our problem in a missing data framework. We denote the *observed data* as $\{\mathcal{D}_i = (X_i, R_i, R_i Y_i)\}_{i=1}^{n+N}$, where R_i is a binary indicator that indicates whether observation \mathcal{D}_i is labeled ($R_i = 1$), or unlabeled ($R_i = 0$). We let $\mathcal{D} = (X, R, RY)$ denote an independent

copy of $\mathcal{D}_i = (X_i, R_i, R_i Y_i)$. We denote the data-generating distribution as $\mathbb{P}^* \in \mathcal{D}$, where \mathcal{D} is the set of distributions induced by a nonparametric model, and thus we write $\mathcal{D} \sim \mathbb{P}^*$. For theoretical convenience, we also define the *full data* $\mathcal{D}^F = (X, Y)$, that is, the data that we would observe if there were no missingness mechanisms in place.

The potential discrepancy between the labeled and unlabeled datasets due to *distribution shift* naturally leads us to adopt a *missing at random* (MAR) labeling mechanism. Moreover, a distinctive aspect of our setting is that the proportion of labeled data n may become asymptotically negligible compared to the volume of unlabeled data N . Specifically, we consider the extreme regime in which $\lim_{n, N \rightarrow \infty} n/(n+N) = 0$. This scenario effectively violates the standard assumption of *positivity*, typically required in classical missing data analyses, where the ratio $n/(n+N)$ is always bounded away from zero. By defining the *propensity score* as $\pi_{n, N}^*(x) = \mathbb{P}[R = 1 | X = x]$, we can formally state these assumptions below.

Assumption 2.1 (D^2S^3 setting). Let the following assumptions hold:

- a. **Missing at random.** $R \perp\!\!\!\perp Y | X$.
- b. **Decaying overlap.** Given $a_{n, N}^{-1} = \mathbb{E}[\pi_{n, N}^{*-1}(X)] < \infty$ for every n and N , it holds that $a_{n, N} > 0$, with potentially $a_{n, N} \rightarrow 0$ as $n, N \rightarrow \infty$.

Remark 2.2. Assumption **a** corresponds to the well-known *ignorability* condition, commonly invoked in both the missing data and causal inference literature (Kennedy, 2024; Tsiatis, 2006). Unlike classical semi-supervised settings that assume labels are missing completely at random (MCAR), our setup allows for selection bias, or distribution shift, in the labeled data. As a result, population-level parameters cannot be consistently estimated using the labeled sample alone. The goal of our work is not merely to enhance supervised estimators using additional unlabeled data (which are no longer unbiased under MAR), but rather to construct a theoretically grounded estimator of general functionals of the full data-generating process. Assumption **b**, inspired by the asymptotic framework of Zhang et al. (2023b), formalizes the regime under which our theoretical guarantees are derived. In contrast to much of the existing literature, which assumes strong overlap (i.e., a uniformly bounded away from zero labeling propensity), we allow for overlap to decay with the sample size, requiring new tools to characterize convergence rates in this more general setting.

Remark 2.3 (Triangular arrays). The *propensity score* $\pi_{n, N}^*(x) = \mathbb{P}[R = 1 | X = x]$ plays a central role in our theoretical development under decaying overlap. In particular, Assumption **b** imposes structural constraints on the behavior of $\pi_{n, N}^*$, by allowing it to depend on the sample sizes n and N . A canonical example of the regime of decaying overlap captured by Assumption 2.1 is the MCAR case, in which the propensity score reduces to $\pi_{n, N}^*(x) = n/(n+N)$ for all $x \in \mathbb{R}^p$, implying that $a_{n, N} = n/(n+N)$ in this special case. Hence, both R_i and $\pi_{n, N}^*(X_i)$ form *triangular arrays* over n, N and i , but we suppress the dependence of R_i on n, N for notational simplicity.

Throughout this paper, we focus on the identification and estimation of a target quantity $\theta^* \in \mathbb{R}^q$ that is defined as the Euclidean functional solving $\theta^* = \theta(\mathbb{P}^*)$, with $\theta : \mathcal{D} \rightarrow \mathbb{R}^q$. We restrict our attention to target parameters that could be estimated using *regular* and *asymptotically linear full-data* estimators, that is, targets that admit the expansion

$$\sqrt{n+N}(\hat{\theta}^F - \theta^*) = (n+N)^{-1/2} \sum_{i=1}^{n+N} \varphi^F(\mathcal{D}_i^F; \theta^*) + o_{\mathbb{P}}(1), \quad (1)$$

for some regular and asymptotically linear *full-data* estimator $\hat{\theta}^F$, and some function $\varphi^F(\mathcal{D}_i^F; \theta^*)$, referred to as *full-data influence function*, evaluating the contribution of the *full-data* observation \mathcal{D}_i^F to the overall estimator $\hat{\theta}^F$ (Hampel, 1974). The influence function $\varphi^F(\mathcal{D}_i^F; \theta^*)$ depends on the true parameter θ^* and is such that $\mathbb{E}[\varphi^F(\mathcal{D}^F; \theta^*)] = 0$ and $\mathbb{V}[\varphi^F(\mathcal{D}^F; \theta^*)]$ is positive definite. This framework is very general and encompasses M-estimation, Z-estimation, U-statistics, and many estimands in causal inference. Examples of such targets are the outcome mean, the outcome quantiles, least squares coefficients, average treatment effects, and general minimizers of convex loss functions depending on both X and Y (Tsiatis, 2006; Van der Vaart, 2000).

There is a deep connection between regular and asymptotically linear estimators and influence functions – see Theorem 3.1 in Tsiatis (2006). In fact, given a full-data influence function $\varphi^F(\mathcal{D}^F; \theta^*)$, one can recover the associated estimator $\hat{\theta}^F$ by solving the estimating equation

$$\sum_{i=1}^{n+N} \varphi^F(\mathcal{D}_i^F; \theta^*) = 0. \quad (2)$$

Standard semiparametric theory guarantees that, under mild conditions, the classical estimator $\hat{\theta}^F$ characterized in Equation 1 and Equation 2 is consistent for θ^* and asymptotically normal. This follows from well-known properties of influence functions and an application of the Central Limit Theorem. The asymptotic variance of the estimator $\hat{\theta}^F$ is given by the variance of its influence function divided by the sample size, i.e. $\mathbb{V}[\varphi^F(\mathcal{D}^F; \theta^*)]/(n+N)$. Notice that if we do not make assumptions on the distribution of the data-generating process, we are left with a problem that is inherently nonparametric. In this case, semiparametric theory shows that each functional is associated with one and only one full-data influence function, and thus it is also the efficient one (i.e. the one delivering the smallest asymptotic variance).

While convenient from a theoretical standpoint, the full-data estimator $\hat{\theta}^F$ is of little practical relevance, as it relies on outcome labels that are missing in the unlabeled portion of the data. A natural first approximation is to construct an estimator using only the labeled sample. However, under the missing at random (MAR) assumption, such an estimator is generally biased due to distribution shifts in the labeling mechanism. Our objective is therefore to understand *how* to construct an unbiased and asymptotically normal estimator for the target parameter θ^* , using the observed data $\mathcal{D} = (X, R, RY)$ in the presence of decaying overlap. We then develop a general and flexible strategy for constructing estimators that remain valid under this challenging regime.

2.1 Notation

Before proceeding, we introduce some more notation. We denote *weak convergence* of a random object Z_n to a limit Z as $Z_n \rightsquigarrow Z$. Similarly, we denote *convergence in \mathbb{L}^p norm* as $Z_n \xrightarrow{\mathbb{L}^p} Z$. Given a random object Z_n , we denote its variance as $\mathbb{V}[Z_n]$. If Z_n is q -dimensional, then $\mathbb{V}[Z_n]$ must be understood as a $q \times q$ positive definite variance-covariance matrix. We also define the \mathbb{L}_p norm of a q -dimensional vector Z as $\|Z\|_p = \left(\sum_{j=1}^q Z_j^p\right)^{1/p}$. Given a $q \times q$ matrix A , $\lambda_{\min}(A)$ and $\lambda_{\max}(A)$ indicate its smallest and largest eigenvalues, respectively. The $q \times q$ identity matrix is denoted as I_q . 0_q denotes a vector of size q whose entries are all zeros. For any two sequences a_n and b_n , we write $a_n \asymp b_n$ if there exist constants c, C, n_0 such that $cb_n < a_n < Cb_n$ for all $n > n_0$.

3 Learning in the D^2S^3 setting

3.1 Known propensity score model

In this Section, we develop results for estimation and inference in the D^2S^3 setting under the assumption that the propensity score $\pi_{n,N}^*$ is known. This setup is particularly relevant in experimental designs where the labeling mechanism is controlled and fully specified, but resources for treatment administration are scarce.

When outcome labels are missing at random, the full-data estimator defined in Equation 1 is not directly computable, as it relies on unobserved outcomes in the unlabeled sample. To properly account for the MAR mechanism, we derive the *observed-data influence function*, which is the projection of the full-data influence function onto the observed data model (Tsiatis, 2006). Under the D^2S^3 setting in

Assumption 2.1, the observed-data influence function for the target θ^* is given by:

$$\begin{aligned}\varphi(\mathcal{D}; \theta^*) &= \frac{R}{\pi_{n,N}^*(X)} \varphi^F(\mathcal{D}; \theta^*) - \frac{R - \pi_{n,N}^*(X)}{\pi_{n,N}^*(X)} \mathbb{E}[\varphi^F(\mathcal{D}; \theta^*) | X] \\ &= \mathbb{E}[\varphi^F(\mathcal{D}; \theta^*) | X] + \frac{R}{\pi_{n,N}^*(X)} (\varphi^F(\mathcal{D}; \theta^*) - \mathbb{E}[\varphi^F(\mathcal{D}; \theta^*) | X]),\end{aligned}\tag{3}$$

where $\varphi^F(\mathcal{D}; \theta^*)$ is any valid full-data influence function, and $\pi_{n,N}^* : \mathbb{R}^p \rightarrow (0, 1)$ denotes the propensity score, defined as $\pi_{n,N}^*(x) = \mathbb{P}[R = 1 | X = x]$. The derivation of this result is detailed in Supplementary Material Section A.

In Equation 3, the only unknown component is the *nuisance function* $\mu^*(X) = \mathbb{E}[\varphi^F(\mathcal{D}; \theta^*) | X]$, which we refer to as the *projection model*. In fact, for the moment, we assume that the propensity score is known, and this amounts to assume that $\hat{\pi} = \pi_{n,N}^*$. To make the dependence on nuisance functions explicit, we denote the influence function evaluated at $\hat{\mu}$ and $\hat{\pi}$ as $\varphi(\mathcal{D}; \theta^*; \hat{\mu}; \hat{\pi})$. In particular, the observed-data influence function where $\hat{\mu} = \mu^*$ and $\hat{\pi} = \pi_{n,N}^*$ is denoted as $\varphi(\mathcal{D}; \theta^*; \mu^*; \pi_{n,N}^*)$.

Since μ^* must be estimated from the data, we employ *cross-fitting* to avoid restrictive Donsker conditions and to retain full-sample efficiency (Bickel and Ritov, 1988; Chernozhukov et al., 2018; Robins et al., 2008; Schick, 1986; Zheng and Van Der Laan, 2010). Cross-fitting works as follows. We first randomly split the observations $\{\mathcal{D}_1, \dots, \mathcal{D}_{n+N}\}$ into J disjoint folds (without loss of generality, we assume that the number of observations $n + N$ is divisible by J). For each $j = 1, \dots, J$ we form $\hat{\mathbb{P}}^{[-j]}$ with all but the j -th fold, and we denote the set of indices of the observations belonging to the j -th fold as $\mathcal{X}^{[j]} \subseteq \{1, \dots, n + N\}$. Then, we learn $\hat{\mu}^{[-j]}$ on $\hat{\mathbb{P}}^{[-j]}$. For most supervised methods, learning $\hat{\mu}^{[-j]}$ on $\hat{\mathbb{P}}^{[-j]}$ will involve using only labeled observations within $\hat{\mathbb{P}}^{[-j]}$. Then, we compute the estimator $\hat{\theta}_\mu$ by solving the estimating equation

$$\sum_{j=1}^J \sum_{i \in \mathcal{X}^{[j]}} \varphi(\mathcal{D}_i; \theta^*; \hat{\mu}^{[-j]}; \pi_{n,N}^*) = 0.\tag{4}$$

Estimating the true projection function μ^* can be challenging in practice, especially when the number of labeled samples is limited. However, due to *double robustness*, the estimator derived from Equation 4 remains consistent and asymptotically normal even when $\hat{\mu}$ is misspecified, as long as it converges to some limit $\bar{\mu} \neq \mu^*$ (in a sense we will make precise shortly). The cost of such misspecification is an increase in asymptotic variance relative to the case where $\hat{\mu} = \mu^*$.

We can now state some regularity conditions needed to show the theoretical properties of our estimators.

Assumption 3.1 (Inference). Let the number of cross-fitting folds be fixed at J , and assume that:

- a. There exist $\bar{\mu}$ and $\bar{\pi}_{n,N}$ such that, for each $j \in \{1, \dots, J\}$, one has

$$\varphi(\mathcal{D}; \theta^*; \hat{\mu}^{[-j]}; \hat{\pi}^{[-j]}) \xrightarrow{\mathbb{L}^2} \varphi(\mathcal{D}; \theta^*; \bar{\mu}; \bar{\pi}_{n,N}).\tag{5}$$

- b. For each $j \in \{1, \dots, J\}$, one has

$$(n + N)^{1/2} a_{n,N}^{1/2} \sum_{j=1}^J \|\eta^{[j]}\|_2 = o_{\mathbb{P}}(1),\tag{6}$$

where the *remainder term* $\eta^{[j]}$ is defined as $\eta^{[j]} = \theta(\hat{\mathbb{P}}^{[-j]}) - \theta(\mathbb{P}^*) + \mathbb{E}[\varphi(\mathcal{D}; \theta^*; \hat{\mu}^{[-j]}; \hat{\pi}^{[-j]})]$.

- c. $\lambda_{\min}(\mathbb{V}[\varphi(\mathcal{D}; \theta^*; \bar{\mu}; \bar{\pi}_{n,N})]) \asymp a_{n,N}^{-1}$ and $\lambda_{\max}(\mathbb{V}[\varphi(\mathcal{D}; \theta^*; \bar{\mu}; \bar{\pi}_{n,N})]) \asymp a_{n,N}^{-1}$.

- d. For every $\varepsilon > 0$, it holds that

$$\mathbb{E} \left[a_{n,N} \|\varphi(\mathcal{D}; \theta^*; \bar{\mu}; \bar{\pi}_{n,N})\|_2^2 \mathbb{1} \left\{ \|\varphi(\mathcal{D}; \theta^*; \bar{\mu}; \bar{\pi}_{n,N})\|_2 > \varepsilon \sqrt{\frac{n+N}{a_{n,N}}} \right\} \right] \rightarrow 0 \quad \text{as } n, N \rightarrow \infty.\tag{7}$$

Remark 3.2. Fixing the number of cross-fitting folds prevents undesirable asymptotic behavior and is standard in modern semiparametric literature. Assumptions **a** and **b** are also conventional; see, for example, [Kennedy \(2024\)](#). Assumption **a** is used to control the empirical process fluctuations, while Assumption **b** ensures that the remainder term in the *von Mises expansion* is negligible. Assumptions **c** and **d** restrict the class of admissible targets within our framework, while still allowing for a broad and general set of results. Specifically, Assumption **c** imposes a condition on the scaling of the asymptotic variance of the influence function, whereas Assumption **d** introduces a technical requirement on the rate at which the observed-data influence function decays with the sample sizes n and N . This latter condition is motivated by the classical Lindeberg condition, which is commonly assumed in proving Central Limit Theorems (CLTs), and is in fact close to being necessary for asymptotic normality. Our formulation generalizes the analogous condition used by [Zhang et al. \(2023b\)](#) to accommodate a wider class of targets. In particular, we recover Assumption 3.2 of [Zhang et al. \(2023b\)](#) by noticing that, for a univariate target (and thus a unidimensional influence function), the norm in Assumption **d** reduces to the absolute value of the influence function itself.

Remark 3.3 (Lindeberg condition). At first glance, Assumption **d** may appear benign: as $n, N \rightarrow \infty$, the term $a_{n,N} \rightarrow 0$, which might suggest that the Lindeberg-type condition becomes increasingly easy to satisfy. However, this is not the case. A key subtlety lies in the fact that the observed-data influence function $\varphi(\mathcal{D}; \theta^*)$ is itself a function of n and N , particularly through its dependence on the labeling mechanism and the propensity scores. This introduces a non-trivial coupling between the behavior of the influence function and the rate $a_{n,N}$. As $a_{n,N} \rightarrow 0$, the weights applied to individual observations in the influence function increase, especially in regions of the covariate space where the propensity score is small. Consequently, while the factor $a_{n,N}$ in the condition vanishes, the tails of the influence function may become heavier due to extreme reweighting. This interplay can make the Lindeberg condition more delicate – not less. In this sense, the condition acts as a technical safeguard that balances asymptotic variance control with tail robustness under decaying overlap.

We are now ready to provide our first result, characterizing the asymptotic behavior of our estimators with known propensity score under the D^2S^3 setting.

Theorem 3.4 (Consistency and asymptotic normality, known $\pi_{n,N}^*$). *Assume $(n + N)a_{n,N} \rightarrow \infty$ and that $\pi_{n,N}^*$ is known. Under Assumption 2.1 (D^2S^3 setting) and Assumptions 3.1 (inference) **a**, **c**, and **d**, one has*

$$(n + N)^{1/2} a_{n,N}^{1/2} \|\hat{\theta}_{\hat{\mu}} - \theta^*\|_2 = O_{\mathbb{P}}(1), \quad (8)$$

and

$$(n + N)^{1/2} \mathbb{V} \left[\varphi \left(\mathcal{D}; \theta^*; \hat{\mu}; \pi_{n,N}^* \right) \right]^{-1/2} (\hat{\theta}_{\hat{\mu}} - \theta^*) \rightsquigarrow \mathcal{N}(0, I_q). \quad (9)$$

Remark 3.5 (Effective sample size). The quantity $(n + N)a_{n,N}$ can be interpreted as the *effective sample size* that governs the convergence rate of the estimator $\hat{\theta}_{\hat{\mu}}$ to the target parameter θ^* . The factor $a_{n,N}$ reflects the severity of overlap decay, by capturing both how concentrated the propensity score $\pi_{n,N}^*$ is around zero and the relative size of the labeled dataset n . The greater the concentration of $\pi_{n,N}^*$ near zero, the slower the rate of convergence. In the special case where labels are missing completely at random (MCAR), we have $\pi_{n,N}^*(x) = n/(n + N)$ for all $x \in \mathbb{R}^p$, which implies $a_{n,N} = n/(n + N)$ and thus an effective sample size equal to n . In this regime, the rate of convergence reduces to the standard root- n rate typically achieved when using labeled data alone. Our findings align with asymptotic results established in [Angelopoulos et al. \(2023b\)](#) and [Xu et al. \(2025\)](#).

3.2 Unknown propensity score model

In general observational studies, both the projection model μ^* and the propensity score $\pi_{n,N}^*$ are unknown and need to be estimated. We employ again *cross-fitting*. We randomly split the observations $\{\mathcal{D}_1, \dots, \mathcal{D}_{n+N}\}$ into J disjoint folds. For each $j = 1, \dots, J$ we form $\hat{\mu}^{[-j]}$ with all but the j -th fold, and we denote the set of indices of the observations belonging to the j -th fold as $\mathcal{K}^{[j]} \subseteq \{1, \dots, n + N\}$.

Then, we learn $\hat{\mu}^{[-j]}$ and $\hat{\pi}^{[-j]}$ on $\hat{\rho}^{[-j]}$, and compute the estimator $\hat{\theta}_{\hat{\mu};\hat{\pi}}$ by solving the estimating equation

$$\sum_{j=1}^J \sum_{i \in \mathcal{X}^{[j]}} \varphi(\mathcal{D}_i; \theta^*; \hat{\mu}^{[-j]}; \hat{\pi}^{[-j]}) = 0. \quad (10)$$

We can now extend the results of Theorem 3.4 to the more general case where all nuisance functions are estimated from the data.

Theorem 3.6 (Consistency and asymptotic normality, unknown nuisances). *Assume $(n+N)a_{n,N} \rightarrow \infty$. Under Assumption 2.1 (D^2S^3 setting) and Assumptions 3.1 (inference) **a**, **b**, **c**, and **d**, one has*

$$(n+N)^{1/2} a_{n,N}^{1/2} \|\hat{\theta}_{\hat{\mu};\hat{\pi}} - \theta^*\|_2 = O_{\mathbb{P}}(1), \quad (11)$$

and

$$(n+N)^{1/2} \mathbb{V}[\varphi(\mathcal{D}; \theta^*; \hat{\mu}; \hat{\pi})]^{-1/2} (\hat{\theta}_{\hat{\mu};\hat{\pi}} - \theta^*) \rightsquigarrow \mathcal{N}(0, I_q). \quad (12)$$

Remark 3.7 (Asymptotic normality under misspecification). When both the projection model and the propensity score are correctly specified, Theorem 3.6 ensures that $\hat{\theta}_{\hat{\mu};\hat{\pi}}$ is asymptotically normal. The consistency of the estimator relies on the remainder term η vanishing asymptotically, as required by Assumption 3.1, part **b**. Algebraically, this remainder is driven by the product of the errors of the nuisance functions, scaling with $\|\hat{\pi} - \pi_{n,N}^*\|_2 \|\hat{\mu} - \mu^*\|_2$. Therefore, Assumption **b** implicitly requires that at least one of the two nuisance models is correctly specified (*double robustness*). If both models are misspecified, this condition generally fails, and consistency is lost. Furthermore, if only one component is correctly specified, achieving asymptotic normality is more demanding, as the correctly specified nuisance function must converge at the faster rate of $(n+N)^{-1/2} a_{n,N}^{-1/2}$, which is typically attainable *only* when its population counterpart belongs to a low-dimensional, parametric model class. Therefore, in complex applications, the relaxation of Assumption **b** may inhibit asymptotic normality and preserve only consistency.

3.3 Prediction-powered inference in the D^2S^3 setting

In this Section, we extend the framework developed so far to incorporate additional information from an off-the-shelf predictive model f that maps the covariate space to the outcome space. We do not impose assumptions on the quality of f , treating it as a generic black-box machine learning prediction model. This extension connects naturally to the *prediction-powered inference* (PPI) framework introduced by [Angelopoulos et al. \(2023a\)](#), but significantly broadens its applicability in real-world scientific settings.

In particular, while the original PPI framework assumes that labels are missing completely at random (MCAR), our extension relaxes this to the more general missing at random (MAR) setting, where the labeling mechanism may depend on the covariates. Additionally, while the original PPI framework is limited to M -estimation problems, our approach supports any target functional satisfying Equation 1. As a result, our formulation enables the use of predictive models within PPI even under covariate-dependent labeling, allowing the benefits of modern machine learning to be realized in more realistic and challenging scenarios. Notably, standard PPI methods are not valid under MAR.

As in previous Sections, we recast the problem in the language of missing data. The observed data are now given by $\mathcal{D} = (X, f(X), R, RY)$, with $n+N$ realizations. In this context, the observed-data influence function for PPI takes the form:

$$\varphi^{\text{PPI}}(\mathcal{D}; \theta^*) = \frac{R}{\pi_{n,N}^*(X, f(X))} \varphi^F(\mathcal{D}; \theta^*) - \frac{R - \pi_{n,N}^*(X, f(X))}{\pi_{n,N}^*(X, f(X))} \mathbb{E}[\varphi^F(\mathcal{D}; \theta^*) | X, f(X)]. \quad (13)$$

All results presented in the previous Sections extend naturally to this setting. The key distinction is that both the projection model and the propensity score can now be conditional on the additional covariate

$f(X)$, which is always observed and may improve the quality of both nuisance estimates. In particular, we can establish consistency and asymptotic normality for the resulting PPI estimator $\hat{\theta}^{\text{PPI}}$, obtained by solving the associated estimating equation involving the influence function in Equation 13, under the D^2S^3 setting.

Corollary 3.8 (PPI asymptotic normality under D^2S^3 setting). *Assume $(n + N)a_{n,N} \rightarrow \infty$. Under Assumption 2.1 (D^2S^3 setting) and Assumption 3.1 (inference), one has*

$$(n + N)^{1/2} a_{n,N}^{1/2} \|\hat{\theta}^{\text{PPI}} - \theta^*\|_2 = O_{\mathbb{P}}(1), \quad (14)$$

and

$$(n + N)^{1/2} \mathbb{V}[\varphi^{\text{PPI}}(\mathcal{D}; \theta^*; \hat{\mu}; \hat{\pi})]^{-1/2} (\hat{\theta}^{\text{PPI}} - \theta^*) \rightsquigarrow \mathcal{N}(0, I_q). \quad (15)$$

Remark 3.9. The utility of incorporating an external predictive model f into the estimation procedure – as in the PPI framework – depends critically on the information that $f(X)$ carries relative to the covariates X . In many practical applications, f is a deterministic function, such as a black-box machine learning predictor trained externally. In this case, $f(X)$ is entirely determined by X , and the conditional expectations in Equation 3 project the full-data influence function $\varphi^F(\mathcal{D}^F; \theta^*)$ onto the same σ -field as in the original setting. As a result, the asymptotic variance of the resulting estimator remains unchanged, and the inclusion of f does not yield a theoretical efficiency gain – though it can still offer great practical advantages by simplifying nuisance model specification. More interesting behavior arises when f introduces additional randomness or knowledge beyond X . Many modern models (e.g., variational autoencoders, Bayesian methods, and transformers) produce a predictive distribution rather than a single deterministic point estimate; as a result, multiple valid predictions $f(X)$ may be associated with the same covariates X . In such cases, the σ -field onto which the conditional expectations project the full-data influence function may change, and the augmented variable $f(X)$ can reduce the residual variance by capturing information orthogonal to X , especially if it correlates with omitted features influencing the outcome.

Finally, we note that our framework can naturally accommodate the integration of multiple predictive models; that is, we can simultaneously leverage a collection of off-the-shelf models $\{f_1, \dots, f_m\}$ within our estimation procedure, allowing us to flexibly combine information from diverse sources and enhance robustness in practical applications (Shan et al., 2025).

4 Simulation study

In this Section, we instantiate the general theory developed above for two specific target parameters: the *multivariate outcome mean* and the *coefficients of a linear regression model*. For each case, we conduct extensive simulation studies to assess the finite-sample performance of the proposed estimators under varying degrees of overlap and model misspecifications. We compare our estimators to a *naive* estimator computed only on the labeled dataset, the *outcome regression* (OR) and the *inverse probability weighting* (IPW) counterparts. The OR influence function is

$$\varphi^{\text{OR}}(\mathcal{D}; \theta^*) = \mathbb{E}[\varphi^F(\mathcal{D}; \theta^*) | X], \quad (16)$$

while the IPW influence function is

$$\varphi^{\text{IPW}}(\mathcal{D}; \theta^*) = \frac{R}{\pi_{n,N}^*(X)} \varphi^F(\mathcal{D}; \theta^*). \quad (17)$$

We employ cross-fitting to learn nuisance functions involved in the computation of our estimator, OR and IPW, with $J = 2$ folds.

We are interested in probing double robustness and measuring actual coverage. Therefore, we assess performance in terms of estimation accuracy, inferential coverage, and inferential power. To measure accuracy, we compute the root mean squared error under the \mathbb{L}_2 -distance between the true $\theta^* \in \mathbb{R}^q$ and

its estimate $\hat{\theta}$, i.e. $\text{RMSE}[\hat{\theta}] = \|\hat{\theta} - \theta^*\|_2$. To measure coverage, we evaluate the empirical fraction of times Δ in which each component of $\hat{\theta}^*$ falls into the asymptotic rectangular region defined by the $1 - \alpha$ coordinate-wise confidence intervals of $\hat{\theta}$. To measure power, we compute the average width of the $1 - \alpha$ coordinate-wise confidence intervals for each component of θ^* . In Supplementary Material Section C, we also report simulation results for simultaneous confidence regions.

We mimic and extend the data-generating process in the simulation study conducted by Zhang et al. (2023b). For each $i = 1, \dots, n + N$, we first generate p -dimensional i.i.d. Gaussian covariates $X_i \sim \mathcal{N}(0, I_p)$. Then we assign the missingness label according to a Bernoulli law, i.e. $R_i | X_i \sim \text{Ber}(\pi_{n,N}^*(X_i))$, where the propensity score $\pi_{n,N}^*$ is modeled as:

- *Decaying MCAR*. The labeled indices are selected uniformly at random, implying $\pi_{n,N}^*(X_i) = n/(n + N)$.
- *Decaying logistic*. The selection probabilities are set to $\pi_{n,N}^*(X_i) = \text{expit}(\log(n/(n + N)) + X_i^T \gamma)$ where $\text{expit}(x) = \exp(x)/(1 + \exp(x))$. The vector of coefficients γ is defined as $\gamma = (1, -1, 0_{p-2})$. This setting corresponds to a logistic propensity score with *decaying offset* (see Supplementary Figure C.1 for a graphical illustration).

We then generate outcomes $Y_i \in \mathbb{R}^k$ according to the following linear model:

$$Y_i = \beta^T X_i + \varepsilon_i, \quad (18)$$

where $\beta \in \mathbb{R}^{p \times k}$, $\beta_\ell \sim \mathcal{N}(0, I_p)$ for each $\ell = 1, \dots, k$, and $\varepsilon_i \sim \mathcal{N}(0, 0.1 \cdot I_k)$.

We model the propensity score using a constant estimator, which essentially corresponds to a MCAR estimator, and an offset logistic regression. Within each fold j , the constant estimator computes $\sum_{i \in \hat{\mathcal{P}}^{[j]}} R_i / |\hat{\mathcal{P}}^{[j]}|$, while the offset in the logistic regression is set at $\log(\sum_{i \in \hat{\mathcal{P}}^{[j]}} R_i / |\hat{\mathcal{P}}^{[j]}|)$. Similarly, we model the outcome regression using either a constant model (mean) or linear regression. For each simulation scenario, we set $\alpha = 0.05$, $p = 10$, $n \in \{100, 500, 1000\}$, $N \in \{10n, 100n\}$. Each configuration is replicated across 1000 random seeds.

4.1 Multivariate outcome mean

Given full data $\mathcal{D}^F = (X, Y)$, with $X \in \mathbb{R}^p$ and $Y \in \mathbb{R}^k$, the k -dimensional full-data influence function for the k -dimensional target parameter $\theta^* = \mathbb{E}[Y]$ is

$$\varphi^F(\mathcal{D}^F; \theta^*) = Y - \theta^*. \quad (19)$$

The observed data are $\mathcal{D} = (X, R, RY)$, and thus the observed-data influence function takes the form

$$\varphi(\mathcal{D}; \theta^*) = \mu^*(X) + \frac{R}{\pi_{n,N}^*(X)} (Y - \mu^*(X)) - \theta^*, \quad (20)$$

where $\mu^* : \mathbb{R}^p \rightarrow \mathbb{R}^k$ is equal to $\mathbb{E}[Y | X]$. The previous influence function motivates the well-known *augmented inverse probability weighting* (AIPW) estimator (Bang and Robins, 2005)

$$\hat{\theta}_{\hat{\mu}, \hat{\pi}}^{\text{AIPW}} = \frac{1}{n + N} \sum_{j=1}^J \sum_{i \in \mathcal{X}^{[j]}} \left[\hat{\mu}^{[-j]}(X_i) + \frac{R_i}{\hat{\pi}^{[-j]}(X_i)} (Y_i - \hat{\mu}^{[-j]}(X_i)) \right]. \quad (21)$$

Similarly, the naive, OR and IPW (Rosenbaum and Rubin, 1983) estimators for the multivariate outcome mean are:

$$\hat{\theta}^{\text{naive}} = \frac{1}{\sum_{i=1}^{n+N} R_i} \sum_{i=1}^{n+N} R_i Y_i, \quad \hat{\theta}_{\hat{\mu}}^{\text{OR}} = \frac{1}{n + N} \sum_{j=1}^J \sum_{i \in \mathcal{X}^{[j]}} \hat{\mu}^{[-j]}(X_i), \quad \hat{\theta}_{\hat{\pi}}^{\text{IPW}} = \frac{1}{n + N} \sum_{j=1}^J \sum_{i \in \mathcal{X}^{[j]}} \frac{R_i Y_i}{\hat{\pi}^{[-j]}(X_i)}. \quad (22)$$

Here, we set $k = 2$, so that the problem becomes bivariate outcome mean estimation. Figure 1 reports results for the decaying logistic scenario with $n = 100$ labeled samples and $N = 1000$ unlabeled samples,

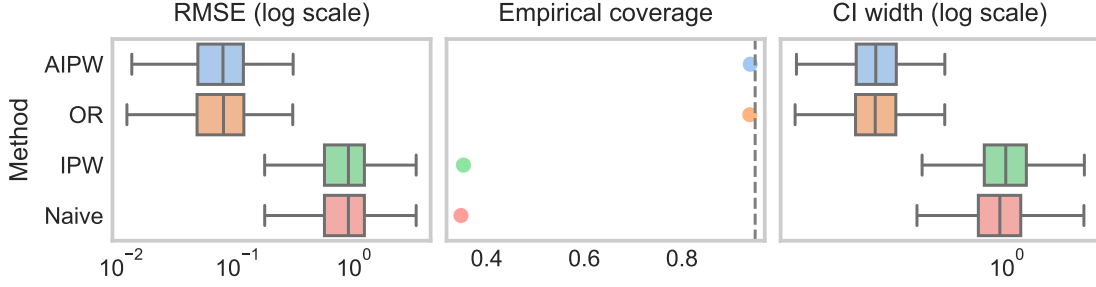


Figure 1: Multivariate outcome mean simulation results. The simulation is run 1000 times under the decaying logistic scenario with $n = 100$ labeled samples and $N = 1000$ unlabeled samples; the outcome model $\hat{\mu}$ is estimated using linear regression, and propensity score model $\hat{\pi}$ is estimated via constant estimator. The left panel displays boxplots summarizing the RMSE distribution over different seeds of the considered estimators. The central panel shows empirical coverage. The right panel displays the distribution of the width of the confidence intervals over different seeds.

the outcome model $\hat{\mu}$ estimated using linear regression, and propensity score model $\hat{\pi}$ estimated via constant estimator. All the other simulation results are reported in Supplementary Material Section C. The boxplot of RMSE shows that both our AIPW proposal and OR achieve low and stable error across replications, while IPW, using a misspecified nuisance function, exhibits bias. Similarly, the naive estimator, which does not adjust for distribution shift, performs poorly. The central and right panels confirm these trends in terms of coverage: our approach and OR attain near-nominal coverage (around 95%) with “narrow” confidence intervals, while IPW and the naive estimator suffer from substantial undercoverage despite the wider confidence intervals. These results highlight the robustness and efficiency of AIPW under the D^2S^3 regime. Similar conclusions can be drawn by analyzing other simulation scenarios in Supplementary Material Section C.

4.2 Linear regression coefficients

Given full data $\mathcal{D}^F = (X, Y)$, with $X \in \mathbb{R}^p$ and $Y \in \mathbb{R}$, the p -dimensional full-data influence function for the p -dimensional target parameter $\theta^* = \operatorname{argmin}_{\theta} \mathbb{E}[(Y - X^T \theta)^2]$ is

$$\varphi^F(\mathcal{D}^F; \theta^*) = \Sigma_X^{-1} X (Y - X^T \theta^*), \quad (23)$$

where $\Sigma_X = \mathbb{E}[XX^T] \in \mathbb{R}^{p \times p}$. The observed data are $\mathcal{D} = (X, R, RY)$, and thus the observed-data influence function takes the form

$$\varphi(\mathcal{D}; \theta^*) = \Sigma_X^{-1} X \mu^*(X) + \frac{R}{\pi_{n,N}^*(X)} \Sigma_X^{-1} X (Y - \mu^*(X)) - \Sigma_X^{-1} X X^T \theta^*, \quad (24)$$

where $\mu^* : \mathbb{R}^p \rightarrow \mathbb{R}$ is equal to $\mathbb{E}[Y | X]$. We estimate the nuisance $\mathbb{E}[XX^T]$ at a parametric rate, i.e. $(n+N)^{-1/2}$, using the covariates in both the labeled and unlabeled datasets via the sample covariance $\hat{\Sigma} = (n+N)^{-1} \sum_{i=1}^{n+N} X_i X_i^T$. The previous influence function motivates the *augmented inverse probability weighting* (AIPW) estimator

$$\hat{\theta}_{\hat{\mu}; \hat{\pi}}^{\text{AIPW}} = \hat{\Sigma}^{-1} \frac{1}{n+N} \sum_{j=1}^J \sum_{i \in \mathcal{X}^{[j]}} X_i \left[\hat{\mu}^{[-j]}(X_i) + \frac{R_i}{\hat{\pi}^{[-j]}(X_i)} (Y_i - \hat{\mu}^{[-j]}(X_i)) \right]. \quad (25)$$

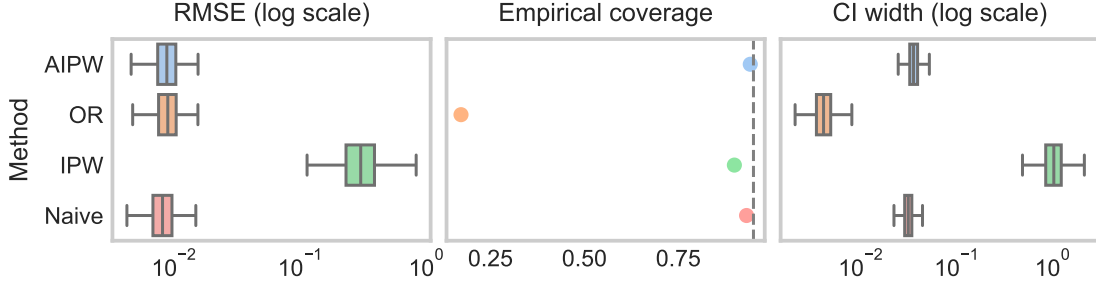


Figure 2: Linear regression coefficients simulation results. The simulation is run 1000 times under the decaying logistic scenario with $n = 100$ labeled samples and $N = 1000$ unlabeled samples; the outcome model $\hat{\mu}$ is estimated using linear regression, and propensity score model $\hat{\pi}$ is estimated via constant estimator. The left panel displays boxplots summarizing the RMSE distribution over different seeds of the considered estimators. The central panel shows empirical coverage. The right panel displays the distribution of the width of the confidence intervals over different seeds.

Similarly, the naive, OR and IPW estimators for the linear regression coefficients are:

$$\hat{\theta}^{\text{naive}} = \left(\frac{1}{\sum_{i=1}^{n+N} R_i} \sum_{i=1}^{n+N} R_i X_i X_i^T \right)^{-1} \frac{1}{\sum_{i=1}^{n+N} R_i} \sum_{i=1}^{n+N} X_i R_i Y_i, \quad \hat{\theta}_{\hat{\mu}}^{\text{OR}} = \hat{\Sigma}^{-1} \frac{1}{n+N} \sum_{j=1}^J \sum_{i \in \mathcal{X}^{(j)}} X_i \hat{\mu}^{[-j]}(X_i),$$

$$\hat{\theta}_{\hat{\pi}}^{\text{IPW}} = \hat{\Sigma}^{-1} \frac{1}{n+N} \sum_{j=1}^J \sum_{i \in \mathcal{X}^{(j)}} X_i \frac{R_i Y_i}{\hat{\pi}^{[-j]}(X_i)}.$$
(26)

Figure 2 presents results for the decaying logistic scenario ($n = 100$, $N = 1000$) where the outcome model $\hat{\mu}$ is estimated via linear regression and the propensity score $\hat{\pi}$ via a constant estimator. In terms of estimation accuracy, the RMSE boxplots show that all estimators except IPW achieve low and stable error. The IPW estimator, relying on a misspecified propensity model, performs poorly, exhibiting both higher bias and variability. The analysis of inferential properties (central and right panels) reveals a critical limitation of pure outcome regression in this setting. The OR estimator displays extremely low coverage despite its high accuracy; because $\hat{\mu}$ is well-specified, the residuals vanish, resulting in artificially narrow confidence intervals that fail to account for the intrinsic noise of the outcome. Conversely, the biased IPW estimator approximately attains correct coverage because its substantial variance inflates the confidence interval widths. The proposed AIPW estimator effectively resolves this trade-off, inheriting the high estimation precision of OR while recovering the valid inferential coverage of IPW. We also note that the naive estimator remains valid in this setting, as the conditional distribution of Y given X is invariant under MAR (Little, 1992; Moon et al., 2025). These findings underscore the robustness of AIPW under decaying overlap; additional scenarios supporting these conclusions are detailed in Supplementary Material Section C.

5 Real-data applications

5.1 BLE-RSSI study

To demonstrate the practical utility of our approach, we first apply it to the BLE-RSSI dataset (Mohammadi et al., 2017). This dataset was collected in a library using Received Signal Strength Indicator (RSSI) measurements obtained from an array of 13 Bluetooth Low Energy (BLE) iBeacons. Data acquisition was performed using a smartphone during the library’s operational hours. The primary objective motivating this dataset is to enable indoor localization, that is, to accurately estimate the spatial position of a mobile device based on wireless signal strength measurements, a key problem in many real-world applications

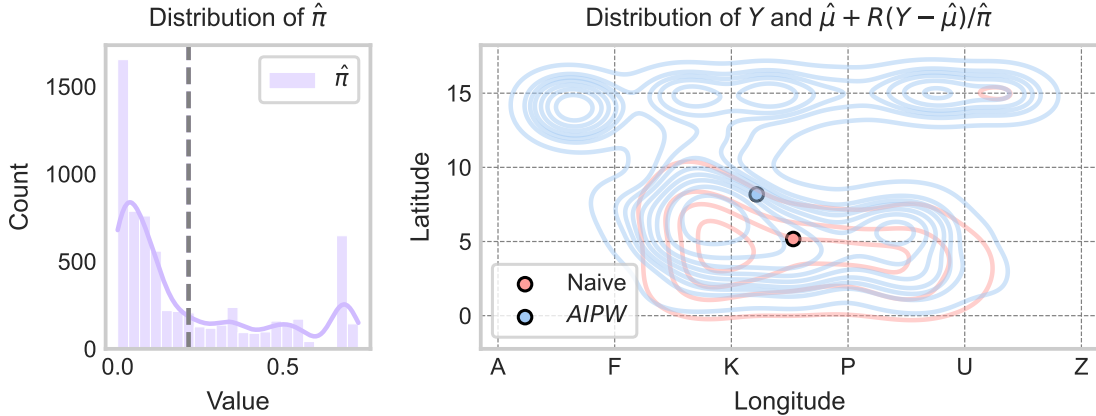


Figure 3: BLE-RSSI application results. Left panel: estimated propensity scores across observations, along with the proportion of labeled data $n/(n+N)$, shown as a vertical dashed line. The heterogeneity in the estimated propensity scores may suggest a missing-at-random (MAR) labeling mechanism. Right panel: joint bivariate distribution over the floor bivariate grid of the observed position of the device Y (red) compared to the distribution of pseudo-outcomes (blue), that is augmented predicted positions from the estimated outcome model using signal recorded by remote sensors. The discrepancy between observed and predicted outcomes may suggest a missing-at-random (MAR) labeling mechanism. Dots represent bivariate means computed using our AIPW approach and the naive approach.

including navigation, resource management, and smart building systems.

The dataset comprises two components: a labeled subset containing $n = 1420$ observations and an unlabeled subset containing $N = 5191$ observations. For each labeled observation, the recorded features include a location identifier and the RSSI readings from the 13 iBeacons. Location identifiers combine a letter (representing longitude) and a number (representing latitude) within the physical layout of the floor. A schematic diagram illustrating the arrangement of the iBeacons and the labeled locations is provided in Supplementary Material Figure D.2. Each location label is then mapped to a two-dimensional real-valued coordinate, representing the longitude and latitude of the device at the time of measurement.

The inferential goal in this application is to estimate the mean spatial position of the device across the observed population. Thus, the problem can be formulated as one of bivariate outcome mean estimation, where the target parameter is the mean of a two-dimensional random vector. Formally, let $Y_i \in \mathbb{R}^2$ denote the bivariate spatial coordinates (longitude and latitude) for observation i ; $R_i \in \{0, 1\}$ indicate whether the location label is observed; and $X_i \in \mathbb{R}^p$ represent the vector of $p = 13$ RSSI readings from the iBeacons, used as auxiliary covariates. The observed data take the form $\mathcal{D}_i = (X_i, R_i, R_i Y_i)$, for $i = 1, \dots, n+N$.

We compare two estimation strategies: the naive estimator, which only uses labeled observations and ignores selection bias, and the AIPW estimator defined in Equation 21, which corrects for the semi-supervised structure. For the AIPW estimator, the outcome regression function $\hat{\mu}$ is estimated using random forests (Breiman, 2001), with RSSI measurements as predictors. The propensity score $\hat{\pi}$ is estimated using logistic regression with offset, also based on RSSI predictors. To mitigate overfitting and ensure valid asymptotic properties, both nuisance functions are estimated using cross-fitting with $J = 5$ folds.

Results are presented in Figure 3. The heterogeneous distribution of the estimated propensity scores indicates that the probability of label observation varies across the covariate space, supporting the plausibility of a missing-at-random (MAR) assumption conditional on the RSSI features. Furthermore, the distribution of the pseudo-outcomes, i.e. the spatial coordinates $\hat{\mu} + R(Y - \hat{\mu})/\hat{\pi}$ shows a marked shift

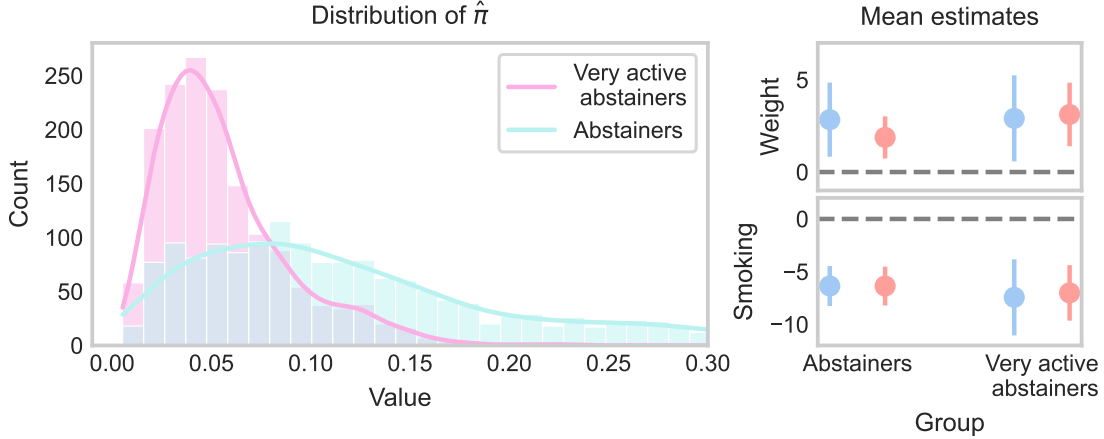


Figure 4: NHEFS application results. Left panel: estimated propensity scores across observations, for various missingness indicators (very active, moderately active, marginal). The heterogeneity in the estimated propensity scores may suggest a missing-at-random (MAR) labeling mechanism. Right panel: estimated means from AIPW (blue) and the naive estimator based solely on labeled data (red). Confidence intervals are at $\alpha = 0.05$ significance level.

compared to the labeled outcomes Y , moving upward and to the left in the two-dimensional grid. This discrepancy between the labeled and imputed outcome distributions highlights the necessity of properly accounting for the semi-supervised structure of the data. Ignoring the unlabeled data or treating the labeled set as representative would likely introduce substantial bias in the estimation of the mean device position. Overall, this example demonstrates how the proposed methodology can successfully leverage partially labeled data to produce robust and unbiased inference in complex real-world settings.

5.2 NHEFS study

We further apply our method to the *National Health and Nutrition Examination Survey Data I Epidemiologic Follow-up Study* (NHEFS). The NHEFS was jointly initiated by the National Center for Health Statistics and the National Institute on Aging to investigate relationships between clinical, nutritional, and behavioral factors.

Following [Ertefaie et al. \(2023\)](#); [Hernán and Robins \(2010\)](#); [Zhang et al. \(2023a\)](#), we consider a subset of the NHEFS which consists of 1561 smokers aged 25-74, who had a first baseline visit and a second follow-up visit approximately 10 years later. Our goal is to estimate the mean for two outcomes of interest: weight change and smoking intensity change. We thus formulate this problem as bivariate outcome mean estimation. To simulate a challenging semi-supervised setting with distribution shift, we define the labeled set based on alcohol consumption. Specifically, we treat observations as labeled ($R_i = 1$) only if the participant abstains from alcohol, while drinkers are treated as unlabeled observations ($R_i = 0$). This creates a scenario where the labeled mechanism is sparse (approximately 12.5% of the data are labeled, i.e. $n = 195$ and $N = 1366$) and likely biased, as abstainers may differ systematically from the general population in terms of health behaviors. When observed, the response variable $Y_i \in \mathbb{R}^2$ contains weight change and smoking intensity change; while the always observed $X_i \in \mathbb{R}^p$ contains $p = 9$ demographic and health covariates, including baseline weight, age, sex, race, education, exercise and activity habits, years of smoking, and whether the individual has quit smoking between the two visits. We compare the naive estimator (sample mean of labeled data) against the AIPW estimator defined in Equation 21. As in the previous application, we estimate the nuisance function $\hat{\mu}$ using random forests ([Breiman, 2001](#)) and the propensity score $\hat{\pi}$ using logistic regression with an offset, employing 5-fold cross-fitting.

Results are presented in Figure 4. On the labeled dataset, the naive estimator suggests a mean weight gain of $1.88kg$. Although not significantly different, the AIPW estimator appears to correct for the distribution shift, estimating a higher population mean weight gain of $2.34kg$. This suggests that the labeled sub-population (alcohol abstainers) may experience less weight gain than the general population, a bias our method identifies and corrects. The results for the change in smoking intensity seem to agree between the two estimators, with AIPW estimating a reduction of -6.36 cigarettes per day.

To empirically validate our theoretical findings regarding decaying overlap, we further stratify the dataset by activity level. In particular, we only consider the cohort of “very active” individuals as labeled. This subset comprises only $n = 89$ subjects (approximately 5.7% of the entire dataset). In this regime, the AIPW estimator remains stable with reasonable standard errors. In fact, the estimated weight change is $2.91kg$, compared to the naive estimate of $3.12kg$. Similarly, for the change in smoking intensity, the AIPW estimator reports a reduction of -7.44 cigarettes per day, while the naive estimator suggests a reduction of -7.01 . The left panel of Figure 4 illustrates the distribution of the estimated propensity scores for this subgroup, which are concentrated near zero (mostly < 0.15), reflecting the severe sparsity of the labeled data. Despite this challenging regime ($n/N \approx 0.057$), the estimator yields informative 95% confidence intervals $- [0.58, 5.24]$ for weight gain and $[-11.05, -3.82]$ for smoking reduction – confirming that our method maintains inferential validity even under significant label scarcity. The divergence between the naive and AIPW estimates indicates that the “very active” labeled cohort is systematically different from the general population; specifically, the naive estimator appears to overestimate weight gain and underestimate smoking reduction, a bias that our approach detects and corrects by properly weighting the unlabeled data.

6 Conclusions

In this work, we have developed a general semiparametric framework for estimation and inference in semi-supervised learning problems where outcome labels are missing at random (MAR) and the overlap decays with sample size. Our approach accommodates arbitrary statistical targets and remains valid under flexible modeling of high-dimensional nuisance functions. Leveraging the tools of semiparametric theory, we have derived influence functions under decaying overlap and shown that AIPW estimators preserve double robustness and asymptotically normality.

A key insight of our analysis is that overlap decay imposes fundamental adaptations of inference, invalidating classical root- n asymptotics and requiring a redefinition of the effective sample size. We formally characterized this rate through a generalization of Lindeberg conditions and provided practical AIPW estimators that remain consistent in this more challenging regime. We further extended our methodology to incorporate black-box prediction models in the spirit of prediction-powered inference (PPI), broadening its applicability to MAR labeling mechanisms.

Our simulation studies confirmed the theoretical properties of AIPW estimators in the D^2S^3 setting, including double robustness, asymptotic normality, and valid coverage under finite samples and severe overlap decay. These findings suggest that our framework is both theoretically sound and practically useful, especially in settings where labeled data are scarce and distribution shift is non-negligible.

Despite these contributions, several limitations remain. First, while we allow for decaying overlap and general targets, our current framework assumes that the MAR assumption holds, i.e., distribution shift depends only on covariates and not on unobserved variables. Relaxing this assumption toward a missing-not-at-random (MNAR) setting would require substantially different identification strategies. Second, the performance of AIPW estimators under strong model misspecification remains to be fully understood. Lastly, while we allow for high-dimensional covariates and flexible machine learning models, our theoretical guarantees rely on sufficient regularity and convergence rates that may be difficult to verify or achieve in practice.

Future research directions include extending our theory to MNAR mechanisms and exploring adaptive procedures that optimize the bias-variance trade-off in regions of low overlap. Another important

direction is the integration of these techniques into large-scale machine learning pipelines for high-throughput scientific applications, such as genomic association studies, fairness-aware recommendation systems, and policy evaluation in digital platforms.

By relaxing traditional assumptions while preserving rigorous inferential guarantees, our work provides a foundation for reliable statistical inference in the increasingly common regime of biased labeling and partial supervision.

Acknowledgments

L.T. wishes to thank Francesca Chiaromonte and Edward H. Kennedy for very helpful discussions. This project was funded by National Institute of Mental Health (NIMH) grant R01MH123184.

References

- Anastasios N Angelopoulos, Stephen Bates, Clara Fannjiang, Michael I Jordan, and Tijana Zrnic. Prediction-powered inference. *Science*, 382(6671):669–674, 2023a.
- Anastasios N Angelopoulos, John C Duchi, and Tijana Zrnic. Ppi++: Efficient prediction-powered inference. *arXiv preprint arXiv:2311.01453*, 2023b.
- David Azriel, Lawrence D Brown, Michael Sklar, Richard Berk, Andreas Buja, and Linda Zhao. Semi-supervised linear regression. *Journal of the American Statistical Association*, 117(540):2238–2251, 2022.
- Heejung Bang and James M Robins. Doubly robust estimation in missing data and causal inference models. *Biometrics*, 61(4):962–973, 2005.
- Richard Berk, Lawrence Brown, Andreas Buja, Kai Zhang, and Linda Zhao. Valid post-selection inference. *The Annals of Statistics*, pages 802–837, 2013.
- Peter J Bickel and Yaacov Ritov. Estimating integrated squared density derivatives: sharp best order of convergence estimates. *Sankhyā: The Indian Journal of Statistics, Series A*, pages 381–393, 1988.
- Peter J Bickel, Chris AJ Klaassen, Ya’acov Ritov, and Jon A Wellner. *Efficient and adaptive estimation for semiparametric models*, volume 4. Springer, 1993.
- Leo Breiman. Random forests. *Machine learning*, 45:5–32, 2001.
- T Cai and Zijian Guo. Semisupervised inference for explained variance in high dimensional linear regression and its applications. *Journal of the Royal Statistical Society Series B: Statistical Methodology*, 82(2):391–419, 2020.
- Jacob Carlson and Melissa Dell. A unifying framework for robust and efficient inference with unstructured data. *arXiv preprint arXiv:2505.00282*, 2025.
- Abhishek Chakraborty, Guorong Dai, and Raymond J Carroll. Semi-supervised quantile estimation: Robust and efficient inference in high dimensional settings. *arXiv preprint arXiv:2201.10208*, 2022.
- Olivier Chapelle, Bernhard Scholkopf, and Alexander Zien. Semi-supervised learning (chapelle, o. et al., eds.; 2006)[book reviews]. *IEEE Transactions on Neural Networks*, 20(3):542–542, 2009.
- Yi-Hau Chen and Hung Chen. A unified approach to regression analysis under double-sampling designs. *Journal of the Royal Statistical Society Series B: Statistical Methodology*, 62(3):449–460, 2000.
- Li-Hsin Cheng, Te-Cheng Hsu, and Che Lin. Integrating ensemble systems biology feature selection and bimodal deep neural network for breast cancer prognosis prediction. *Scientific Reports*, 11(1):14914, 2021.

- Victor Chernozhukov, Denis Chetverikov, Mert Demirer, Esther Duflo, Christian Hansen, Whitney Newey, and James Robins. Double/debiased machine learning for treatment and structural parameters. *The Econometrics Journal*, pages C1–C68, 2018.
- David R Cox. Regression models and life-tables. *Journal of the Royal Statistical Society: Series B (Methodological)*, 34(2):187–202, 1972.
- Richard K Crump, V Joseph Hotz, Guido W Imbens, and Oscar A Mitnik. Dealing with limited overlap in estimation of average treatment effects. *Biometrika*, 96(1):187–199, 2009.
- Christina Curtis, Sohrab P Shah, Suet-Feung Chin, Gulisa Turashvili, Oscar M Rueda, Mark J Dunning, Doug Speed, Andy G Lynch, Shamith Samarajiwa, Yinyin Yuan, et al. The genomic and transcriptomic architecture of 2,000 breast tumours reveals novel subgroups. *Nature*, 486(7403):346–352, 2012.
- Alexander D’Amour, Peng Ding, Avi Feller, Lihua Lei, and Jasjeet Sekhon. Overlap in observational studies with high-dimensional covariates. *Journal of Econometrics*, 221(2):644–654, 2021.
- Ashkan Ertefaie, Nima S Hejazi, and Mark J van der Laan. Nonparametric inverse-probability-weighted estimators based on the highly adaptive lasso. *Biometrics*, 79(2):1029–1041, 2023.
- Chakravarthy Garlapati, Shriya Joshi, Shristi Bhattarai, Jayashree Krishnamurthy, Ravi Chakra Turaga, Thi Nguyen, Xiaoxian Li, and Ritu Aneja. Plk1 and aurkb phosphorylate survivin differentially to affect proliferation in racially distinct triple-negative breast cancer. *Cell Death & Disease*, 14(1):12, 2023.
- Frank R Hampel. The influence curve and its role in robust estimation. *Journal of the american statistical association*, 69(346):383–393, 1974.
- Miguel A Hernán and James M Robins. Causal inference, 2010.
- Te-Cheng Hsu and Che Lin. Learning from small medical data—robust semi-supervised cancer prognosis classifier with bayesian variational autoencoder. *Bioinformatics Advances*, 3(1):vbac100, 2023.
- Wenlong Ji, Lihua Lei, and Tijana Zrnic. Predictions as surrogates: Revisiting surrogate outcomes in the age of ai. *arXiv preprint arXiv:2501.09731*, 2025.
- Edward H Kennedy. Semiparametric doubly robust targeted double machine learning: a review. *Handbook of Statistical Methods for Precision Medicine*, pages 207–236, 2024.
- Shakeeb Khan and Elie Tamer. Irregular identification, support conditions, and inverse weight estimation. *Econometrica*, 78(6):2021–2042, 2010.
- Rae-Kwon Kim, Yongjoon Suh, Ki-Chun Yoo, Yan-Hong Cui, Hyeonmi Kim, Min-Jung Kim, In Gyu Kim, and Su-Jae Lee. Activation of kras promotes the mesenchymal features of basal-type breast cancer. *Experimental & molecular medicine*, 47(1):e137–e137, 2015.
- Dan M Kluger, Kerri Lu, Tijana Zrnic, Sherrie Wang, and Stephen Bates. Prediction-powered inference with imputed covariates and nonuniform sampling. *arXiv preprint arXiv:2501.18577*, 2025.
- Arun K Kuchibhotla, John E Kolassa, and Todd A Kuffner. Post-selection inference. *Annual Review of Statistics and Its Application*, 9(1):505–527, 2022.
- Roderick JA Little. Regression with missing x’s: a review. *Journal of the American statistical association*, 87(420):1227–1237, 1992.
- Jiacheng Miao, Xinran Miao, Yixuan Wu, Jiwei Zhao, and Qiongshi Lu. Assumption-lean and data-adaptive post-prediction inference. *arXiv preprint arXiv:2311.14220*, 2023.
- Mehdi Mohammadi, Ala Al-Fuqaha, Mohsen Guizani, and Jun-Seok Oh. Semisupervised deep reinforcement learning in support of iot and smart city services. *IEEE Internet of Things Journal*, 5(2):624–635, 2017.

- Haeun Moon, Jin-Hong Du, Jing Lei, and Kathryn Roeder. Augmented doubly robust post-imputation inference for proteomic data. *bioRxiv*, pages 2024–03, 2025.
- Bernard Pereira, Suet-Feung Chin, Oscar M Rueda, Hans-Kristian Moen Vollan, Elena Provenzano, Helen A Bardwell, Michelle Pugh, Linda Jones, Roslin Russell, Stephen-John Sammut, et al. The somatic mutation profiles of 2,433 breast cancers refine their genomic and transcriptomic landscapes. *Nature communications*, 7(1):11479, 2016.
- James Robins, Lingling Li, Eric Tchetgen, Aad van der Vaart, et al. Higher order influence functions and minimax estimation of nonlinear functionals. In *Probability and statistics: essays in honor of David A. Freedman*, volume 2, pages 335–422. Institute of Mathematical Statistics, 2008.
- Paul R Rosenbaum and Donald B Rubin. The central role of the propensity score in observational studies for causal effects. *Biometrika*, 70(1):41–55, 1983.
- Christoph Rothe. Robust confidence intervals for average treatment effects under limited overlap. *Econometrica*, 85(2):645–660, 2017.
- Anton Schick. On asymptotically efficient estimation in semiparametric models. *The Annals of Statistics*, pages 1139–1151, 1986.
- Jiawei Shan, Yiming Dong, and Jiwei Zhao. Sada: Safe and adaptive inference with multiple black-box predictions. *arXiv preprint arXiv:2509.21707*, 2025.
- Shanshan Song, Yuanyuan Lin, and Yong Zhou. A general m-estimation theory in semi-supervised framework. *Journal of the American Statistical Association*, 119(546):1065–1075, 2024.
- Yoshihisa Tokumaru, Masanori Oshi, Eriko Katsuta, Li Yan, Vikas Satyananda, Nobuhisa Matsuhashi, Manabu Futamura, Yukihiro Akao, Kazuhiro Yoshida, and Kazuaki Takabe. Kras signaling enriched triple negative breast cancer is associated with favorable tumor immune microenvironment and better survival. *American journal of cancer research*, 10(3):897, 2020.
- Anastasios A Tsiatis. *Semiparametric theory and missing data*, volume 4. Springer, 2006.
- Ai Ueda, Keiki Oikawa, Koji Fujita, Akio Ishikawa, Eiichi Sato, Takashi Ishikawa, Masahiko Kuroda, and Kohsuke Kanekura. Therapeutic potential of plk1 inhibition in triple-negative breast cancer. *Laboratory investigation*, 99(9):1275–1286, 2019.
- Aad W Van der Vaart. *Asymptotic statistics*, volume 3. Cambridge university press, 2000.
- Zichun Xu, Daniela Witten, and Ali Shojaie. A unified framework for semiparametrically efficient semi-supervised learning. *arXiv preprint arXiv:2502.17741*, 2025.
- Shu Yang and Peng Ding. Asymptotic inference of causal effects with observational studies trimmed by the estimated propensity scores. *Biometrika*, 105(2):487–493, 2018.
- Anru Zhang, Lawrence D Brown, and T Tony Cai. Semi-supervised inference: General theory and estimation of means. *Annals of Statistics*, 2019.
- Yuqian Zhang and Jelena Bradic. High-dimensional semi-supervised learning: in search of optimal inference of the mean. *Biometrika*, 109(2):387–403, 2022.
- Yuqian Zhang, Abhishek Chakraborty, and Jelena Bradic. The decaying missing-at-random framework: Doubly robust causal inference with partially labeled data. *arXiv preprint arXiv:2305.12789*, 2023a.
- Yuqian Zhang, Abhishek Chakraborty, and Jelena Bradic. Double robust semi-supervised inference for the mean: selection bias under mar labeling with decaying overlap. *Information and Inference: A Journal of the IMA*, 12(3):2066–2159, 2023b.
- Wenjing Zheng and Mark J Van Der Laan. Asymptotic theory for cross-validated targeted maximum likelihood estimation. 2010.
- Xiaojin Jerry Zhu. Semi-supervised learning literature survey. 2005.

Tijana Zrnic and Emmanuel J Candès. Cross-prediction-powered inference. *Proceedings of the National Academy of Sciences*, 121(15):e2322083121, 2024.

Supplementary Material of “Semiparametric semi-supervised learning for general targets under distribution shift and decaying overlap”

A Proofs of main statements

Wherever convenient, integrals and expectations are written in linear functional notation. Thus, instead of $\mathbb{E}[f(X)] = \int f(x) \mathbb{P}(dx)$, we sometimes write $\mathbb{P}[f]$. In particular, we denote the empirical average operator as \mathbb{P}_{n+N} . We also write φ^F to indicate the full-data influence function for notational simplicity.

A.1 Derivation of Equation 3

Given a full-data influence function φ^F , by Theorem 7.2 in Tsiatis (2006), we know that the space of associated observed-data influence functions Λ^\perp is given by

$$\Lambda^\perp = \left\{ \frac{R}{\pi_{n,N}^*(X)} \varphi^F \oplus \Lambda_2 \right\}, \quad (27)$$

where $\Lambda_2 = \{L_2(\mathcal{D}) : \mathbb{E}[L_2(\mathcal{D}) | \mathcal{D}^F] = 0\}$.

By Theorem 10.1 in Tsiatis (2006), for a fixed φ^F , the optimal observed-data influence function among the class in Equation 27 is obtained by choosing

$$L_2(\mathcal{D}) = -\Pi \left(\frac{R}{\pi_{n,N}^*(X)} \varphi^F \mid \Lambda_2 \right), \quad (28)$$

where the operator Π projects the element $R\varphi^F / \pi_{n,N}^*(X)$ onto the space Λ_2 – see Theorem 2.1 in Tsiatis (2006).

Finally, by Theorem 10.2 in Tsiatis (2006), we know that

$$\Pi \left(\frac{R}{\pi_{n,N}^*(X)} \varphi^F \mid \Lambda_2 \right) = \left(\frac{R - \pi_{n,N}^*(X)}{\pi_{n,N}^*(X)} \right) h_2(X) \in \Lambda_2, \quad (29)$$

where $h_2(X) = \mathbb{E}[\varphi^F | X]$. This concludes the derivation.

A.2 Proof of Theorem 3.4

Proof. For simplicity, we show the result for a single cross-fitting fold. In particular, we denote the distribution where $\hat{\mu}$ is trained as $\hat{\mathbb{P}}$ and the distribution where the influence functions are approximated as \mathbb{P}_{n+N} . Similarly, we denote as $\bar{\mu}$ the population limit of $\hat{\mu}$. The propensity score is known, so that $\hat{\pi} = \bar{\pi}_{n,N} = \pi_{n,N}^*$. By Von Mises expansion, we have

$$\begin{aligned} \hat{\theta}_{\hat{\mu}} - \theta^* &= \theta(\hat{\mathbb{P}}) + \mathbb{P}_{n+N} \left[\varphi(\mathcal{D}; \theta^*; \hat{\mu}; \pi_{n,N}^*) \right] - \theta(\mathbb{P}^*) \\ &= (\mathbb{P}_{n+N} - \mathbb{E}) \left[\varphi(\mathcal{D}; \theta^*; \hat{\mu}; \pi_{n,N}^*) \right] + \eta(\hat{\mu}, \mu^*) \\ &= (\mathbb{P}_{n+N} - \mathbb{E}) \left[\varphi(\mathcal{D}; \theta^*; \bar{\mu}; \pi_{n,N}^*) \right] + (\mathbb{P}_{n+N} - \mathbb{E}) \left[\varphi(\mathcal{D}; \theta^*; \hat{\mu}; \pi_{n,N}^*) - \varphi(\mathcal{D}; \theta^*; \bar{\mu}; \pi_{n,N}^*) \right] + \eta(\hat{\mu}, \mu^*) \\ &= \mathbb{P}_{n+N} \left[\varphi(\mathcal{D}; \theta^*; \bar{\mu}; \pi_{n,N}^*) \right] + (\mathbb{P}_{n+N} - \mathbb{E}) \left[\varphi(\mathcal{D}; \theta^*; \hat{\mu}; \pi_{n,N}^*) - \varphi(\mathcal{D}; \theta^*; \bar{\mu}; \pi_{n,N}^*) \right] + \eta(\hat{\mu}, \mu^*), \end{aligned} \quad (30)$$

where $\eta(\hat{\mu}, \mu^*) = \theta(\hat{\mathbb{P}}) - \theta(\mathbb{P}^*) + \mathbb{E} \left[\varphi(\mathcal{D}; \theta^*; \hat{\mu}; \pi_{n,N}^*) \right]$ by definition. We refer to the three elements on the right-hand side respectively as the *influence function term*, the *empirical process term* and the *remainder term*.

Consistency. To prove consistency, we need to show that the norm of each term on the right-hand side is $O_{\mathbb{P}}\left((n+N)^{-1/2}a_{n,N}^{-1/2}\right)$. We do so by analyzing each term separately.

First term (influence function). By definition of influence function, $\mathbb{E}\left[\varphi\left(\mathcal{D}; \theta^*; \bar{\mu}; \pi_{n,N}^*\right)\right] = 0$, and thus the first term has mean zero. We now analyze the variance. Define $\bar{\mathbb{V}}_{\theta^*} = \mathbb{V}\left[\varphi\left(\mathcal{D}; \theta^*; \bar{\mu}; \pi_{n,N}^*\right)\right] = \mathbb{E}\left[\varphi\left(\mathcal{D}; \theta^*; \bar{\mu}; \pi_{n,N}^*\right)\varphi\left(\mathcal{D}; \theta^*; \bar{\mu}; \pi_{n,N}^*\right)^T\right]$. By Assumption 3.1, **c**, we have $\lambda_{\max}(\bar{\mathbb{V}}_{\theta^*}) \asymp a_{n,N}^{-1}$. Therefore, we have

$$\mathbb{E}\left[\left((n+N)^{1/2}a_{n,N}^{1/2}\left\|\mathbb{P}_{n+N}\left[\varphi\left(\mathcal{D}; \theta^*; \bar{\mu}; \pi_{n,N}^*\right)\right]\right\|_2\right)^2\right] = a_{n,N}\|\bar{\mathbb{V}}_{\theta^*}\|_2^2 \leq a_{n,N}q^2\lambda_{\max}(\bar{\mathbb{V}}_{\theta^*}) = O_{\mathbb{P}}(1), \quad (31)$$

which in turn implies $\left\|\mathbb{P}_{n+N}\left[\varphi\left(\mathcal{D}; \theta^*; \bar{\mu}; \pi_{n,N}^*\right)\right]\right\|_2 = O_{\mathbb{P}}\left((n+N)^{-1/2}a_{n,N}^{-1/2}\right)$.

Second term (Empirical process). We need to show that the norm of $(\mathbb{P}_{n+N} - \mathbb{E})\left[\varphi\left(\mathcal{D}; \theta^*; \hat{\mu}; \pi_{n,N}^*\right) - \varphi\left(\mathcal{D}; \theta^*; \bar{\mu}; \pi_{n,N}^*\right)\right]$ is of order $O_{\mathbb{P}}\left((n+N)^{-1/2}a_{n,N}^{-1/2}\right)$. Define $\delta(\mathcal{D}) = \varphi\left(\mathcal{D}; \theta^*; \hat{\mu}; \pi_{n,N}^*\right) - \varphi\left(\mathcal{D}; \theta^*; \bar{\mu}; \pi_{n,N}^*\right) \in \mathbb{R}^q$. Here, we show the stronger result

$$(n+N)^{1/2}a_{n,N}^{1/2}\|(\mathbb{P}_{n+N} - \mathbb{E})[\delta(\mathcal{D})]\|_2 = o_{\mathbb{P}}(1). \quad (32)$$

First, we have:

$$\delta(\mathcal{D}) = \left(1 - \frac{R}{\pi_{n,N}^*(X)}\right)(\hat{\mu}(X) - \bar{\mu}(X)). \quad (33)$$

Conditional on the training fold $\hat{\mathbb{P}}$ (so $\hat{\mu}$ is fixed), this term is a mean zero vector. We now calculate the expected squared Euclidean norm of the scaled empirical process vector $(n+N)^{1/2}a_{n,N}^{1/2}\mathbb{P}_{n+N}[\delta(\mathcal{D})]$ conditional on $\hat{\mathbb{P}}$:

$$\begin{aligned} \mathbb{E}\left[\left\|(n+N)^{1/2}a_{n,N}^{1/2}\mathbb{P}_{n+N}[\delta(\mathcal{D})]\right\|_2^2 \mid \hat{\mathbb{P}}\right] &= \frac{a_{n,N}}{n+N} \sum_{i=1}^{n+N} \mathbb{E}\left[\|\delta(\mathcal{D}_i)\|_2^2 \mid \hat{\mathbb{P}}\right] \\ &= a_{n,N}\mathbb{E}\left[\|\delta(\mathcal{D})\|_2^2 \mid \hat{\mathbb{P}}\right] \\ &= a_{n,N}\mathbb{E}\left[\left(1 - \frac{R}{\pi_{n,N}^*(X)}\right)^2 \|\hat{\mu}(X) - \bar{\mu}(X)\|_2^2 \mid \hat{\mathbb{P}}\right] \\ &= a_{n,N}\mathbb{E}\left[\left(\frac{1}{\pi_{n,N}^*(X)} - 1\right) \|\hat{\mu}(X) - \bar{\mu}(X)\|_2^2 \mid \hat{\mathbb{P}}\right], \end{aligned} \quad (34)$$

where the last equality follows from Lemma B.1. Notice that this term goes to 0 with n going to infinity under Assumption 3.1, **a**. We now apply conditional Chebyshev inequality:

$$\mathbb{P}\left[\left\|(n+N)^{1/2}a_{n,N}^{1/2}\mathbb{P}_{n+N}[\delta(\mathcal{D})]\right\|_2 \geq \varepsilon \mid \hat{\mathbb{P}}\right] \leq \frac{\mathbb{E}\left[\left\|(n+N)^{1/2}a_{n,N}^{1/2}\mathbb{P}_{n+N}[\delta(\mathcal{D})]\right\|_2^2 \mid \hat{\mathbb{P}}\right]}{\varepsilon^2} \rightarrow 0. \quad (35)$$

By taking marginal expectations over the training set, one obtains the desired result.

Third term (Remainder). Again, we need to show that the norm of $\eta(\hat{\mu}, \mu^*)$ equals $O_{\mathbb{P}}\left((n+N)^{-1/2}a_{n,N}^{-1/2}\right)$. This directly follows from the fact the propensity score is known. In fact, by direct evaluation, in this case the remainder term is exactly zero:

$$\begin{aligned} \eta(\hat{\mu}, \mu^*) &= \theta(\hat{\mathbb{P}}) - \theta^* + \mathbb{E}\left[\hat{\mu}(X) + \frac{R}{\pi_{n,N}^*(X)}(\varphi^F(\mathcal{D}; \theta(\hat{\mathbb{P}})) - \hat{\mu}(X))\right] \\ &= \theta(\hat{\mathbb{P}}) - \theta^* + \mathbb{E}\left[\varphi^F(\mathcal{D}; \theta(\hat{\mathbb{P}}))\right] = 0. \end{aligned} \quad (36)$$

The previous results, combined, imply that $\|\hat{\theta}_{\hat{\mu}} - \theta^*\|_2 = O_{\mathbb{P}}\left((n+N)^{-1/2}a_{n,N}^{-1/2}\right)$.

Central Limit Theorem. We now turn to the asymptotic normality of $\hat{\theta}_{\hat{\mu}}$ by showing that the first term on the right-hand side satisfies a form of Central Limit Theorem. This is enough to prove asymptotic normality of the estimator, as the remaining terms are already of order $o_{\mathbb{P}}\left((n+N)^{-1/2}a_{n,N}^{-1/2}\right)$.

By Assumption 3.1, **c**, we have $\lambda_{\min}(\tilde{\mathbb{V}}_{\theta^*}) \asymp a_{n,N}^{-1}$. This implies:

$$\left\|\tilde{\mathbb{V}}_{\theta^*}^{-1/2}\right\|_2^2 = \left(\lambda_{\max}(\tilde{\mathbb{V}}_{\theta^*}^{-1/2})\right)^2 = \left(\lambda_{\min}(\tilde{\mathbb{V}}_{\theta^*})\right)^{-1} \asymp a_{n,N}. \quad (37)$$

By the tail condition **d** in Assumption 3.1, we have that

$$\begin{aligned} & \mathbb{E}\left[\left\|\tilde{\mathbb{V}}_{\theta^*}^{-1/2}\varphi\left(\mathcal{D};\theta^*;\bar{\mu};\pi_{n,N}^*\right)\right\|_2^2 \mathbb{1}\left\{\left\|\tilde{\mathbb{V}}_{\theta^*}^{-1/2}\varphi\left(\mathcal{D};\theta^*;\bar{\mu};\pi_{n,N}^*\right)\right\|_2 > \varepsilon\sqrt{n+N}\right\}\right] \\ & \leq \mathbb{E}\left[\left\|\tilde{\mathbb{V}}_{\theta^*}^{-1/2}\right\|_2^2 \left\|\varphi\left(\mathcal{D};\theta^*;\bar{\mu};\pi_{n,N}^*\right)\right\|_2^2 \mathbb{1}\left\{\left\|\tilde{\mathbb{V}}_{\theta^*}^{-1/2}\right\|_2 \left\|\varphi\left(\mathcal{D};\theta^*;\bar{\mu};\pi_{n,N}^*\right)\right\|_2 > \varepsilon\sqrt{n+N}\right\}\right] \\ & \leq \mathbb{E}\left[C a_{n,N} \left\|\varphi\left(\mathcal{D};\theta^*;\bar{\mu};\pi_{n,N}^*\right)\right\|_2^2 \mathbb{1}\left\{\left\|\sqrt{a_{n,N}}\varphi\left(\mathcal{D};\theta^*;\bar{\mu};\pi_{n,N}^*\right)\right\|_2 > \varepsilon\sqrt{n+N}\right\}\right] \rightarrow 0 \quad \text{as } n, N \rightarrow \infty, \end{aligned} \quad (38)$$

where the first inequality is due to triangle inequality and the second inequality, for some constant $C > 0$, is due to the chain of equalities in Equation 37. Therefore the following Lindeberg condition also holds

$$(n+N)^{-1} \sum_{i=1}^{n+N} \mathbb{E}\left[\left\|\tilde{\mathbb{V}}_{\theta^*}^{-1/2}\varphi\left(\mathcal{D}_i;\theta^*;\bar{\mu};\pi_{n,N}^*\right)\right\|_2^2 \mathbb{1}\left\{\left\|\tilde{\mathbb{V}}_{\theta^*}^{-1/2}\varphi\left(\mathcal{D}_i;\theta^*;\bar{\mu};\pi_{n,N}^*\right)\right\|_2 > \varepsilon\sqrt{n+N}\right\}\right] \rightarrow 0 \quad \text{as } n, N \rightarrow \infty, \quad (39)$$

which implies, by Lindeberg-Feller Central Limit Theorem (Van der Vaart, 2000), that

$$(n+N)^{-1/2}\tilde{\mathbb{V}}_{\theta^*}^{-1/2} \sum_{i=1}^{n+N} \varphi\left(\mathcal{D}_i;\theta^*;\bar{\mu};\pi_{n,N}^*\right) \rightsquigarrow \mathcal{N}\left(0, I_q\right). \quad (40)$$

In summary, we have

$$(n+N)^{1/2}\tilde{\mathbb{V}}_{\theta^*}^{-1/2}\left(\hat{\theta}_{\hat{\mu}} - \theta^*\right) = (n+N)^{-1/2}\tilde{\mathbb{V}}_{\theta^*}^{-1/2} \sum_{i=1}^{n+N} \varphi\left(\mathcal{D}_i;\theta^*;\bar{\mu};\pi_{n,N}^*\right) + o_{\mathbb{P}}(1). \quad (41)$$

□

A.3 Proof of Theorem 3.6

Proof. For simplicity, we show the result for a single cross-fitting fold. In particular, we denote the distribution where $\hat{\mu}$ and $\hat{\pi}$ are trained as $\hat{\mathbb{P}}$ and the distribution where the influence functions are approximated as \mathbb{P}_{n+N} . Similarly, we denote as $\bar{\mu}$ and $\bar{\pi}_{n,N}$ the population limit of $\hat{\mu}$ and $\hat{\pi}$, respectively. By Von Mises expansion, we have

$$\begin{aligned} \hat{\theta}_{\hat{\mu};\hat{\pi}} - \theta^* &= \theta\left(\hat{\mathbb{P}}\right) + \mathbb{P}_{n+N}\left[\varphi\left(\mathcal{D};\theta^*;\hat{\mu};\hat{\pi}\right)\right] - \theta\left(\mathbb{P}^*\right) \\ &= \left(\mathbb{P}_{n+N} - \mathbb{E}\right)\left[\varphi\left(\mathcal{D};\theta^*;\hat{\mu};\hat{\pi}\right)\right] + \eta\left(\left(\hat{\mu}, \hat{\pi}\right), \left(\mu^*, \pi_{n,N}^*\right)\right) \\ &= \left(\mathbb{P}_{n+N} - \mathbb{E}\right)\left[\varphi\left(\mathcal{D};\theta^*;\bar{\mu};\bar{\pi}_{n,N}\right)\right] + \left(\mathbb{P}_{n+N} - \mathbb{E}\right)\left[\varphi\left(\mathcal{D};\theta^*;\hat{\mu};\hat{\pi}\right) - \varphi\left(\mathcal{D};\theta^*;\bar{\mu};\bar{\pi}_{n,N}\right)\right] + \eta\left(\left(\hat{\mu}, \hat{\pi}\right), \left(\mu^*, \pi_{n,N}^*\right)\right) \\ &= \mathbb{P}_{n+N}\left[\varphi\left(\mathcal{D};\theta^*;\bar{\mu};\bar{\pi}_{n,N}\right)\right] + \left(\mathbb{P}_{n+N} - \mathbb{E}\right)\left[\varphi\left(\mathcal{D};\theta^*;\hat{\mu};\hat{\pi}\right) - \varphi\left(\mathcal{D};\theta^*;\bar{\mu};\bar{\pi}_{n,N}\right)\right] + \eta\left(\left(\hat{\mu}, \hat{\pi}\right), \left(\mu^*, \pi_{n,N}^*\right)\right), \end{aligned} \quad (42)$$

where $\eta((\hat{\mu}, \hat{\pi}), (\mu^*, \pi_{n,N}^*)) = \theta(\hat{\mathbb{P}}) - \theta(\mathbb{P}^*) + \mathbb{E}[\varphi(\mathcal{D}; \theta^*; \hat{\mu}; \hat{\pi})]$ by definition. We refer to the three elements on the right-hand side respectively as the *influence function term*, the *empirical process term* and the *remainder term*.

Consistency. To prove consistency, we need to show that the norm of each term on the right-hand side is $O_{\mathbb{P}}\left((n+N)^{-1/2}a_{n,N}^{-1/2}\right)$. We do so by analyzing each term separately.

First term (influence function). By definition of influence function, $\mathbb{E}[\varphi(\mathcal{D}; \theta^*; \bar{\mu}; \bar{\pi}_{n,N})] = 0$, and thus the first term has mean zero. We now analyze the variance. Define $\bar{\mathbb{V}}_{\theta^*} = \mathbb{V}[\varphi(\mathcal{D}; \theta^*; \bar{\mu}; \bar{\pi}_{n,N})] = \mathbb{E}[\varphi(\mathcal{D}; \theta^*; \bar{\mu}; \bar{\pi}_{n,N})\varphi(\mathcal{D}; \theta^*; \bar{\mu}; \bar{\pi}_{n,N})^T]$. By Assumption 3.1, **c**, we have $\lambda_{\max}(\bar{\mathbb{V}}_{\theta^*}) \asymp a_{n,N}^{-1}$. Therefore, we have

$$\mathbb{E}\left[\left((n+N)^{1/2}a_{n,N}^{1/2}\|\mathbb{P}_{n+N}[\varphi(\mathcal{D}; \theta^*; \bar{\mu}; \bar{\pi})]\|_2\right)^2\right] = a_{n,N}\|\bar{\mathbb{V}}_{\theta^*}\|_2^2 \leq a_{n,N}q^2\lambda_{\max}(\bar{\mathbb{V}}_{\theta^*}) = O_{\mathbb{P}}(1), \quad (43)$$

which in turn implies $\|\mathbb{P}_{n+N}[\varphi(\mathcal{D}; \theta^*; \bar{\mu}; \bar{\pi}_{n,N})]\|_2 = O_{\mathbb{P}}\left((n+N)^{-1/2}a_{n,N}^{-1/2}\right)$.

Second term (Empirical process). We need to show that the norm of $(\mathbb{P}_{n+N} - \mathbb{E})[\varphi(\mathcal{D}; \theta^*; \hat{\mu}; \hat{\pi}) - \varphi(\mathcal{D}; \theta^*; \bar{\mu}; \bar{\pi}_{n,N})]$ is of order $O_{\mathbb{P}}\left((n+N)^{-1/2}a_{n,N}^{-1/2}\right)$. Define $\delta(\mathcal{D}) = \varphi(\mathcal{D}; \theta^*; \hat{\mu}; \hat{\pi}) - \varphi(\mathcal{D}; \theta^*; \bar{\mu}; \bar{\pi}_{n,N}) \in \mathbb{R}^q$. Here, we show the stronger result

$$(n+N)^{1/2}a_{n,N}^{1/2}\|(\mathbb{P}_{n+N} - \mathbb{E})[\delta(\mathcal{D})]\|_2 = o_{\mathbb{P}}(1). \quad (44)$$

By definition of the empirical process operator $(\mathbb{P}_{n+N} - \mathbb{E})$, the term $(\mathbb{P}_{n+N} - \mathbb{E})[\delta(\mathcal{D})]$ is centered. We need to focus on the scaled conditional variance, i.e., the scaled expected squared Euclidean norm conditional on $\hat{\mathbb{P}}$:

$$\begin{aligned} \mathbb{E}\left[\left\|(n+N)^{1/2}a_{n,N}^{1/2}(\mathbb{P}_{n+N} - \mathbb{E})[\delta(\mathcal{D})]\right\|_2^2 \mid \hat{\mathbb{P}}\right] &= \frac{a_{n,N}}{n+N} \sum_{i=1}^{n+N} \mathbb{E}[\|\delta(\mathcal{D}_i) - \mathbb{E}[\delta(\mathcal{D})]\|_2^2 \mid \hat{\mathbb{P}}] \\ &= a_{n,N}\mathbb{E}[\|\delta(\mathcal{D}) - \mathbb{E}[\delta(\mathcal{D})]\|_2^2 \mid \hat{\mathbb{P}}] \\ &\leq a_{n,N}\mathbb{E}[\|\delta(\mathcal{D})\|_2^2 \mid \hat{\mathbb{P}}]. \end{aligned} \quad (45)$$

Notice that this term goes to 0 with n going to infinity under Assumption 3.1, **a**. We now apply conditional Chebyshev inequality:

$$\mathbb{P}\left[\left\|(n+N)^{1/2}a_{n,N}^{1/2}(\mathbb{P}_{n+N} - \mathbb{E})[\delta(\mathcal{D})]\right\|_2 \geq \varepsilon \mid \hat{\mathbb{P}}\right] \leq \frac{\mathbb{E}\left[\left\|(n+N)^{1/2}a_{n,N}^{1/2}(\mathbb{P}_{n+N} - \mathbb{E})[\delta(\mathcal{D})]\right\|_2^2 \mid \hat{\mathbb{P}}\right]}{\varepsilon^2} \rightarrow 0. \quad (46)$$

By taking marginal expectations over the training set, one obtains the desired result.

Third term (Remainder). Again, we need to show that the norm of $\eta((\hat{\mu}, \hat{\pi}), (\mu^*, \pi_{n,N}^*))$ equals $O_{\mathbb{P}}\left((n+N)^{-1/2}a_{n,N}^{-1/2}\right)$. This directly follows from Assumption 3.1, **b**.

The previous results, combined, imply that $\|\hat{\theta}_{\hat{\mu}; \hat{\pi}} - \theta^*\|_2 = O_{\mathbb{P}}\left((n+N)^{-1/2}a_{n,N}^{-1/2}\right)$.

Central Limit Theorem. We now turn to the asymptotic normality of $\hat{\theta}_{\hat{\mu}; \hat{\pi}}$ by showing that the first term on the right-hand side satisfies a form of Central Limit Theorem. This is enough to prove asymptotic normality of the estimator, as the remaining terms are already of order $o_{\mathbb{P}}\left((n+N)^{-1/2}a_{n,N}^{-1/2}\right)$.

By Assumption 3.1, **c**, we have $\lambda_{\min}(\bar{\mathbb{V}}_{\theta^*}) \asymp a_{n,N}^{-1}$. This implies:

$$\left\|\bar{\mathbb{V}}_{\theta^*}^{-1/2}\right\|_2^2 = \left(\lambda_{\max}(\bar{\mathbb{V}}_{\theta^*}^{-1/2})\right)^2 = \left(\lambda_{\min}(\bar{\mathbb{V}}_{\theta^*})\right)^{-1} \asymp a_{n,N}. \quad (47)$$

By the tail condition **d** in Assumption 3.1, we have that

$$\begin{aligned}
& \mathbb{E} \left[\left\| \tilde{\mathbb{V}}_{\theta^*}^{-1/2} \varphi(\mathcal{D}; \theta^*; \bar{\mu}; \bar{\pi}_{n,N}) \right\|_2^2 \mathbb{1} \left\{ \left\| \tilde{\mathbb{V}}_{\theta^*}^{-1/2} \varphi(\mathcal{D}; \theta^*; \bar{\mu}; \bar{\pi}_{n,N}) \right\|_2 > \varepsilon \sqrt{n+N} \right\} \right] \\
& \leq \mathbb{E} \left[\left\| \tilde{\mathbb{V}}_{\theta^*}^{-1/2} \right\|_2^2 \left\| \varphi(\mathcal{D}; \theta^*; \bar{\mu}; \bar{\pi}_{n,N}) \right\|_2^2 \mathbb{1} \left\{ \left\| \tilde{\mathbb{V}}_{\theta^*}^{-1/2} \right\|_2 \left\| \varphi(\mathcal{D}; \theta^*; \bar{\mu}; \bar{\pi}_{n,N}) \right\|_2 > \varepsilon \sqrt{n+N} \right\} \right] \\
& \leq \mathbb{E} \left[C a_{n,N} \left\| \varphi(\mathcal{D}; \theta^*; \bar{\mu}; \bar{\pi}_{n,N}) \right\|_2^2 \mathbb{1} \left\{ \left\| \sqrt{a_{n,N}} \varphi(\mathcal{D}; \theta^*; \bar{\mu}; \bar{\pi}_{n,N}) \right\|_2 > \varepsilon \sqrt{n+N} \right\} \right] \rightarrow 0 \quad \text{as } n, N \rightarrow \infty,
\end{aligned} \tag{48}$$

where the first inequality is due to triangle inequality and the second inequality, for some constant $C > 0$, is due to the chain of equalities in Equation 47. Therefore the following Lindeberg condition also holds

$$(n+N)^{-1} \sum_{i=1}^{n+N} \mathbb{E} \left[\left\| \tilde{\mathbb{V}}_{\theta^*}^{-1/2} \varphi(\mathcal{D}_i; \theta^*; \bar{\mu}; \bar{\pi}) \right\|_2^2 \mathbb{1} \left\{ \left\| \tilde{\mathbb{V}}_{\theta^*}^{-1/2} \varphi(\mathcal{D}_i; \theta^*; \bar{\mu}; \bar{\pi}) \right\|_2 > \varepsilon \sqrt{n+N} \right\} \right] \rightarrow 0 \quad \text{as } n, N \rightarrow \infty, \tag{49}$$

which implies, by Lindeberg-Feller Central Limit Theorem (Van der Vaart, 2000), that

$$(n+N)^{-1/2} \tilde{\mathbb{V}}_{\theta^*}^{-1/2} \sum_{i=1}^{n+N} \varphi(\mathcal{D}_i; \theta^*; \bar{\mu}; \bar{\pi}) \rightsquigarrow \mathcal{N}(0, I_q). \tag{50}$$

In summary, we have

$$(n+N)^{1/2} \tilde{\mathbb{V}}_{\theta^*}^{-1/2} (\hat{\theta}_{\hat{\mu}, \hat{\pi}} - \theta^*) = (n+N)^{-1/2} \tilde{\mathbb{V}}_{\theta^*}^{-1/2} \sum_{i=1}^{n+N} \varphi(\mathcal{D}_i; \theta^*; \bar{\mu}; \bar{\pi}_{n,N}) + o_{\mathbb{P}}(1). \tag{51}$$

□

A.4 Proof of Corollary 3.8

Proof. This is a straightforward application of Theorem 3.6, where $f(X)$ is employed as an additional covariate. □

B Additional theoretical results

Here, we provide some high-level conditions that imply Assumption 3.1, **c**, for the multivariate outcome mean target. We assume that the propensity score $\pi_{n,N}^*$ is known, so that $\hat{\pi} = \bar{\pi}_{n,N} = \pi_{n,N}^*$. We first provide a simple yet useful Lemma.

Lemma B.1. *Assume $\hat{\pi} = \bar{\pi}_{n,N} = \pi_{n,N}^*$. Then*

$$\mathbb{E} \left[\left(\frac{R}{\hat{\pi}(X)} - 1 \right)^2 \mid X \right] = \frac{1}{\hat{\pi}(X)} - 1. \tag{52}$$

Proof. The following chain holds:

$$\begin{aligned}
\mathbb{E} \left[\left(\frac{R}{\hat{\pi}(X)} - 1 \right)^2 \mid X \right] &= \mathbb{E} \left[\frac{R^2 + \hat{\pi}^2(X) - 2R\hat{\pi}(X)}{\hat{\pi}^2(X)} \mid X \right] \\
&= \mathbb{E} \left[\frac{R}{\hat{\pi}^2(X)} \mid X \right] + 1 - 2\mathbb{E} \left[\frac{R}{\hat{\pi}(X)} \mid X \right] \\
&= \frac{\mathbb{E}[R \mid X]}{\hat{\pi}^2(X)} + 1 - 2\frac{\mathbb{E}[R \mid X]}{\hat{\pi}(X)} \\
&= \frac{1}{\hat{\pi}(X)} - 1,
\end{aligned} \tag{53}$$

where we are using the facts $R^2 = R$ and $\hat{\pi}(X) = \pi_{n,N}^*(X)$. □

Proposition B.2 (High-level conditions for multivariate outcome mean target). *Let $\theta^* = \mathbb{E}[Y]$ and $\hat{\pi} = \bar{\pi}_{n,N} = \pi_{n,N}^*$. Assume that, for all $\ell = 1, \dots, k$, $\mathbb{E}[(Y_\ell - \mu_\ell^*(X))^2 | X] \geq \sigma_\ell^2$, $\mathbb{E}[(Y_\ell - \bar{\mu}_\ell(X))^2 | X] \leq \bar{\sigma}_\ell^2$ and $\mathbb{V}[Y_\ell] \leq \bar{\sigma}_\ell^2$. Then $\lambda_{\min}(\mathbb{V}[\varphi(\mathcal{D}; \theta^*; \bar{\mu}; \pi_{n,N}^*)]) \asymp a_{n,N}^{-1}$.*

Proof. We first derive additional uniform lower bounds for $\mathbb{E}[(Y_\ell - \bar{\mu}_\ell(X))^2 | X]$ and $\mathbb{V}[Y_\ell]$. By iterated expectation, we have:

$$\begin{aligned} \mathbb{E}[(Y_\ell - \bar{\mu}_\ell(X))^2 | X] &= \mathbb{E}[(Y_\ell - \mu_\ell^*(X) + \mu_\ell^*(X) - \bar{\mu}_\ell(X))^2 | X] \\ &= \mathbb{E}[(Y_\ell - \mu_\ell^*(X))^2 | X] + \mathbb{E}[(\mu_\ell^*(X) - \bar{\mu}_\ell(X))^2 | X] \\ &\quad + 2\mathbb{E}[(Y_\ell - \mu_\ell^*(X))(\mu_\ell^*(X) - \bar{\mu}_\ell(X)) | X] \\ &= \mathbb{E}[(Y_\ell - \mu_\ell^*(X))^2 | X] + \mathbb{E}[(\mu_\ell^*(X) - \bar{\mu}_\ell(X))^2 | X] \\ &\geq \sigma_\ell^2. \end{aligned} \tag{54}$$

Similarly, we can show that:

$$\begin{aligned} \mathbb{V}[Y_\ell] &= \mathbb{E}[(Y_\ell - \mathbb{E}[Y_\ell])^2] \\ &= \mathbb{E}[\mathbb{E}[(Y_\ell - \mu_\ell^*(X))^2 | X] + \mathbb{E}[(\mu_\ell^*(X) - \mathbb{E}[Y_\ell])^2 | X]] \\ &\geq \sigma_\ell^2. \end{aligned} \tag{55}$$

We now show that each diagonal element of $\bar{\mathbb{V}}_{\theta^*}$ is of the same rate as $a_{n,N}^{-1}$. In particular, for each $\ell = 1, \dots, k$ we have:

$$\begin{aligned} \bar{\mathbb{V}}_{\theta^*}[\ell, \ell] &= \mathbb{E}[\varphi(\mathcal{D}; \theta^*; \bar{\mu}; \pi_{n,N}^*)_\ell^2] \\ &= \mathbb{E}\left[\left(\bar{\mu}_\ell(X) + \frac{R(Y_\ell - \bar{\mu}_\ell(X))}{\pi_{n,N}^*(X)} - \mathbb{E}[Y_\ell]\right)^2\right] \\ &= \mathbb{E}\left[\left(\frac{(R - \pi_{n,N}^*(X))(Y_\ell - \bar{\mu}_\ell(X))}{\pi_{n,N}^*(X)} + Y_\ell - \mathbb{E}[Y_\ell]\right)^2\right] \\ &= \mathbb{E}\left[\frac{(R - \pi_{n,N}^*(X))^2}{(\pi_{n,N}^*(X))^2} (Y_\ell - \bar{\mu}_\ell(X))^2\right] + \mathbb{V}[Y_\ell] \\ &= \mathbb{E}\left[\frac{(1 - \pi_{n,N}^*(X))}{\pi_{n,N}^*(X)} (Y_\ell - \bar{\mu}_\ell(X))^2\right] + \mathbb{V}[Y_\ell], \end{aligned} \tag{56}$$

where we are using Lemma B.1. Therefore we have that

$$a_{n,N} \bar{\mathbb{V}}_{\theta^*}[\ell, \ell] \geq a_{n,N} \left(\left(\frac{1}{\pi_{n,N}^*(X)} - 1 \right) \sigma_\ell^2 + \sigma_\ell^2 \right) = \sigma_\ell^2 > 0, \tag{57}$$

and similarly we can show that

$$a_{n,N} \bar{\mathbb{V}}_{\theta^*}[\ell, \ell] \leq a_{n,N} \left(\left(\frac{1}{\pi_{n,N}^*(X)} - 1 \right) \bar{\sigma}_\ell^2 + \bar{\sigma}_\ell^2 \right) = \bar{\sigma}_\ell^2 < \infty. \tag{58}$$

The last two inequalities imply that $\bar{\mathbb{V}}_{\theta^*}[\ell, \ell] \asymp a_{n,N}^{-1}$. We can now exploit Cauchy-Schwartz to expand the previous results to off-diagonal elements of $\bar{\mathbb{V}}_{\theta^*}$. In fact:

$$|\bar{\mathbb{V}}_{\theta^*}[\ell_1, \ell_2]| \leq \sqrt{\bar{\mathbb{V}}_{\theta^*}[\ell_1, \ell_1] \bar{\mathbb{V}}_{\theta^*}[\ell_2, \ell_2]} \asymp a_{n,N}^{-1}. \tag{59}$$

Therefore, for all $\ell_1 = 1, \dots, k$ and $\ell_2 = 1, \dots, k$, it holds that

$$\hat{V}_{\theta^*}[\ell_1, \ell_2] \asymp a_{n,N}^{-1}, \quad (60)$$

which concludes the proof. \square

C Further simulation results

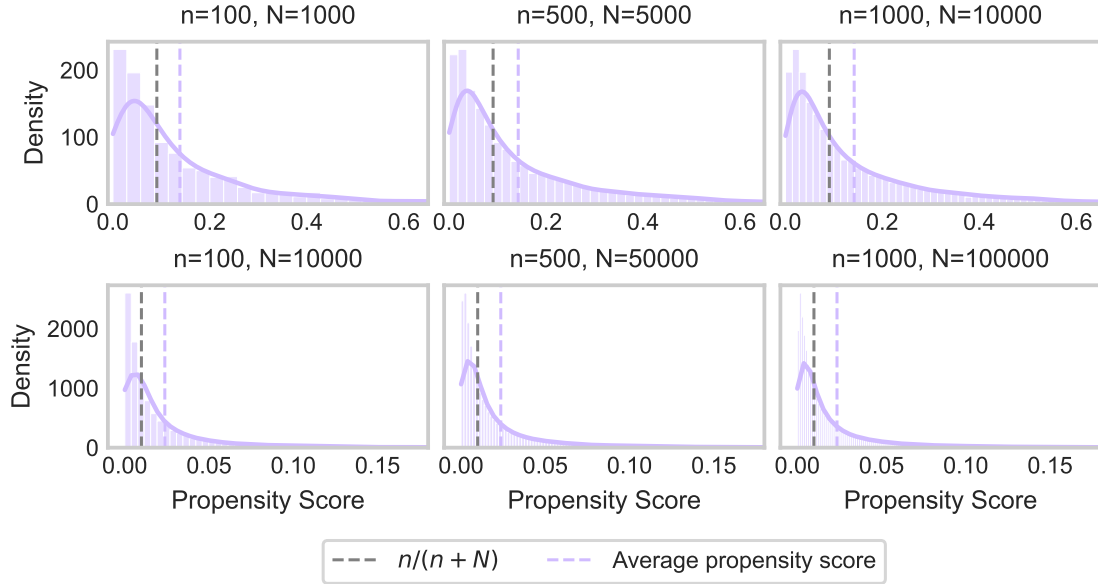


Figure C.1: True propensity score distribution across simulation parameters when the missingness mechanism is governed by a logistic model with offset at $n/(n+N)$. Vertical dashed lines represent empirical average (purple) and theoretical one (grey).

To compute joint coverage, we evaluate the empirical fraction of times Δ in which $\theta^* \in \mathbb{R}^q$ falls into the asymptotic $1 - \alpha$ confidence region of $\hat{\theta}$. In particular, we employ Hotelling one sample T^2 test, which rejects the null hypothesis $\hat{\theta} = \theta^*$ at $1 - \alpha$ level if

$$(\hat{\theta} - \theta^*)^T \hat{V}_{n,N}^{-1} (\hat{\theta} - \theta^*) \geq \frac{q}{n+N-q} F_{q, n+N-q, 1-\alpha}, \quad (61)$$

where $\hat{V}_{n,N}$ is an estimate of the covariance matrix and $F_{q, n+N-q, 1-\alpha}$ is the $1 - \alpha$ quantile of a F -distribution with q and $n+N-q$ degrees of freedom.

n	N	Setting	μ model	π model	AIPW	OR	IPW	Naive
100	1000	Decaying MCAR	Constant	Constant	0.282	0.282	0.282	0.282
100	1000	Decaying MCAR	Constant	Logistic	0.233	0.282	0.216	0.282
100	1000	Decaying MCAR	Linear	Constant	0.081	0.081	0.282	0.282
100	1000	Decaying MCAR	Linear	Logistic	0.082	0.081	0.216	0.282
100	1000	Decaying logistic	Constant	Constant	0.910	0.910	0.910	0.910
100	1000	Decaying logistic	Constant	Logistic	0.683	0.910	0.582	0.910
100	1000	Decaying logistic	Linear	Constant	0.081	0.081	0.910	0.910
100	1000	Decaying logistic	Linear	Logistic	0.086	0.081	0.582	0.910
100	10000	Decaying MCAR	Constant	Constant	0.267	0.267	0.267	0.267
100	10000	Decaying MCAR	Constant	Logistic	0.200	0.267	0.179	0.267
100	10000	Decaying MCAR	Linear	Constant	0.029	0.029	0.267	0.267
100	10000	Decaying MCAR	Linear	Logistic	0.032	0.029	0.179	0.267
100	10000	Decaying logistic	Constant	Constant	1.158	1.158	1.158	1.158
100	10000	Decaying logistic	Constant	Logistic	0.585	1.158	0.492	1.158
100	10000	Decaying logistic	Linear	Constant	0.028	0.028	1.158	1.158
100	10000	Decaying logistic	Linear	Logistic	0.033	0.028	0.492	1.158
500	5000	Decaying MCAR	Constant	Constant	0.123	0.123	0.123	0.123
500	5000	Decaying MCAR	Constant	Logistic	0.045	0.123	0.046	0.123
500	5000	Decaying MCAR	Linear	Constant	0.036	0.036	0.123	0.123
500	5000	Decaying MCAR	Linear	Logistic	0.036	0.036	0.046	0.123
500	5000	Decaying logistic	Constant	Constant	0.868	0.868	0.868	0.868
500	5000	Decaying logistic	Constant	Logistic	0.242	0.868	0.217	0.868
500	5000	Decaying logistic	Linear	Constant	0.036	0.036	0.868	0.868
500	5000	Decaying logistic	Linear	Logistic	0.036	0.036	0.217	0.868
500	50000	Decaying MCAR	Constant	Constant	0.120	0.120	0.120	0.120
500	50000	Decaying MCAR	Constant	Logistic	0.032	0.120	0.031	0.120
500	50000	Decaying MCAR	Linear	Constant	0.013	0.013	0.120	0.120
500	50000	Decaying MCAR	Linear	Logistic	0.014	0.013	0.031	0.120
500	50000	Decaying logistic	Constant	Constant	1.131	1.131	1.131	1.131
500	50000	Decaying logistic	Constant	Logistic	0.228	1.131	0.198	1.131
500	50000	Decaying logistic	Linear	Constant	0.013	0.014	1.131	1.131
500	50000	Decaying logistic	Linear	Logistic	0.014	0.014	0.198	1.131
1000	10000	Decaying MCAR	Constant	Constant	0.087	0.087	0.087	0.087
1000	10000	Decaying MCAR	Constant	Logistic	0.029	0.087	0.030	0.087
1000	10000	Decaying MCAR	Linear	Constant	0.026	0.026	0.087	0.087
1000	10000	Decaying MCAR	Linear	Logistic	0.026	0.026	0.030	0.087
1000	10000	Decaying logistic	Constant	Constant	0.866	0.866	0.866	0.866
1000	10000	Decaying logistic	Constant	Logistic	0.157	0.866	0.142	0.866
1000	10000	Decaying logistic	Linear	Constant	0.026	0.026	0.866	0.866
1000	10000	Decaying logistic	Linear	Logistic	0.026	0.026	0.142	0.866
1000	100000	Decaying MCAR	Constant	Constant	0.085	0.085	0.085	0.085
1000	100000	Decaying MCAR	Constant	Logistic	0.017	0.085	0.016	0.085
1000	100000	Decaying MCAR	Linear	Constant	0.009	0.009	0.085	0.085
1000	100000	Decaying MCAR	Linear	Logistic	0.009	0.009	0.016	0.085
1000	100000	Decaying logistic	Constant	Constant	1.133	1.133	1.133	1.133
1000	100000	Decaying logistic	Constant	Logistic	0.158	1.133	0.137	1.133
1000	100000	Decaying logistic	Linear	Constant	0.009	0.009	1.133	1.133
1000	100000	Decaying logistic	Linear	Logistic	0.010	0.009	0.137	1.133

Table C.1: Multivariate outcome mean simulation results. RMSE is reported for four different estimators. Each row corresponds to a specific configuration of labeled and unlabeled sample sizes, with $n \in \{100, 500, 1000\}$ and $N \in \{10n, 100n\}$, setting, and models for the nuisance functions.

n	N	Setting	μ model	π model	AIPW	OR	IPW	Naive
100	1000	Decaying MCAR	Constant	Constant	0.941	0.037	0.942	0.938
100	1000	Decaying MCAR	Constant	Logistic	1.000	0.037	0.999	0.938
100	1000	Decaying MCAR	Linear	Constant	0.945	0.946	0.942	0.938
100	1000	Decaying MCAR	Linear	Logistic	0.948	0.946	0.999	0.938
100	1000	Decaying logistic	Constant	Constant	0.349	0.011	0.352	0.347
100	1000	Decaying logistic	Constant	Logistic	0.982	0.011	0.974	0.347
100	1000	Decaying logistic	Linear	Constant	0.940	0.939	0.352	0.347
100	1000	Decaying logistic	Linear	Logistic	0.940	0.939	0.974	0.347
100	10000	Decaying MCAR	Constant	Constant	0.953	0.012	0.952	0.948
100	10000	Decaying MCAR	Constant	Logistic	1.000	0.012	1.000	0.948
100	10000	Decaying MCAR	Linear	Constant	0.947	0.933	0.952	0.948
100	10000	Decaying MCAR	Linear	Logistic	0.943	0.933	1.000	0.948
100	10000	Decaying logistic	Constant	Constant	0.221	0.004	0.222	0.220
100	10000	Decaying logistic	Constant	Logistic	0.965	0.004	0.961	0.220
100	10000	Decaying logistic	Linear	Constant	0.940	0.931	0.222	0.220
100	10000	Decaying logistic	Linear	Logistic	0.956	0.931	0.961	0.220
500	5000	Decaying MCAR	Constant	Constant	0.945	0.015	0.945	0.945
500	5000	Decaying MCAR	Constant	Logistic	1.000	0.015	1.000	0.945
500	5000	Decaying MCAR	Linear	Constant	0.957	0.957	0.945	0.945
500	5000	Decaying MCAR	Linear	Logistic	0.957	0.957	1.000	0.945
500	5000	Decaying logistic	Constant	Constant	0.165	0.002	0.165	0.164
500	5000	Decaying logistic	Constant	Logistic	0.976	0.002	0.970	0.164
500	5000	Decaying logistic	Linear	Constant	0.958	0.956	0.165	0.164
500	5000	Decaying logistic	Linear	Logistic	0.959	0.956	0.970	0.164
500	50000	Decaying MCAR	Constant	Constant	0.953	0.005	0.953	0.952
500	50000	Decaying MCAR	Constant	Logistic	1.000	0.005	1.000	0.952
500	50000	Decaying MCAR	Linear	Constant	0.935	0.921	0.953	0.952
500	50000	Decaying MCAR	Linear	Logistic	0.933	0.921	1.000	0.952
500	50000	Decaying logistic	Constant	Constant	0.093	0.000	0.093	0.093
500	50000	Decaying logistic	Constant	Logistic	0.966	0.000	0.959	0.093
500	50000	Decaying logistic	Linear	Constant	0.932	0.927	0.093	0.093
500	50000	Decaying logistic	Linear	Logistic	0.941	0.927	0.959	0.093
1000	10000	Decaying MCAR	Constant	Constant	0.942	0.010	0.941	0.941
1000	10000	Decaying MCAR	Constant	Logistic	1.000	0.010	1.000	0.941
1000	10000	Decaying MCAR	Linear	Constant	0.952	0.951	0.941	0.941
1000	10000	Decaying MCAR	Linear	Logistic	0.954	0.951	1.000	0.941
1000	10000	Decaying logistic	Constant	Constant	0.110	0.001	0.110	0.109
1000	10000	Decaying logistic	Constant	Logistic	0.975	0.001	0.971	0.109
1000	10000	Decaying logistic	Linear	Constant	0.953	0.952	0.110	0.109
1000	10000	Decaying logistic	Linear	Logistic	0.954	0.952	0.971	0.109
1000	100000	Decaying MCAR	Constant	Constant	0.959	0.003	0.960	0.959
1000	100000	Decaying MCAR	Constant	Logistic	1.000	0.003	1.000	0.959
1000	100000	Decaying MCAR	Linear	Constant	0.949	0.933	0.960	0.959
1000	100000	Decaying MCAR	Linear	Logistic	0.950	0.933	1.000	0.959
1000	100000	Decaying logistic	Constant	Constant	0.076	0.000	0.076	0.076
1000	100000	Decaying logistic	Constant	Logistic	0.963	0.000	0.963	0.076
1000	100000	Decaying logistic	Linear	Constant	0.940	0.934	0.076	0.076
1000	100000	Decaying logistic	Linear	Logistic	0.954	0.934	0.963	0.076

Table C.2: Multivariate outcome mean simulation results. Empirical coverage is reported for four different estimators. Each row corresponds to a specific configuration of labeled and unlabeled sample sizes, with $n \in \{100, 500, 1000\}$ and $N \in \{10n, 100n\}$, setting, and models for the nuisance functions.

n	N	Setting	μ model	π model	AIPW	OR	IPW	Naive
100	1000	Decaying MCAR	Constant	Constant	1.224	0.029	1.213	1.207
100	1000	Decaying MCAR	Constant	Logistic	1.800	0.029	1.723	1.207
100	1000	Decaying MCAR	Linear	Constant	0.366	0.364	1.213	1.207
100	1000	Decaying MCAR	Linear	Logistic	0.369	0.364	1.723	1.207
100	1000	Decaying logistic	Constant	Constant	0.957	0.023	0.993	0.949
100	1000	Decaying logistic	Constant	Logistic	3.135	0.023	2.727	0.949
100	1000	Decaying logistic	Linear	Constant	0.365	0.364	0.993	0.949
100	1000	Decaying logistic	Linear	Logistic	0.382	0.364	2.727	0.949
100	10000	Decaying MCAR	Constant	Constant	1.225	0.010	1.213	1.207
100	10000	Decaying MCAR	Constant	Logistic	1.795	0.010	1.717	1.207
100	10000	Decaying MCAR	Linear	Constant	0.129	0.121	1.213	1.207
100	10000	Decaying MCAR	Linear	Logistic	0.137	0.121	1.717	1.207
100	10000	Decaying logistic	Constant	Constant	0.782	0.006	0.837	0.777
100	10000	Decaying logistic	Constant	Logistic	2.636	0.006	2.201	0.777
100	10000	Decaying logistic	Linear	Constant	0.124	0.121	0.837	0.777
100	10000	Decaying logistic	Linear	Logistic	0.147	0.121	2.201	0.777
500	5000	Decaying MCAR	Constant	Constant	0.537	0.006	0.536	0.536
500	5000	Decaying MCAR	Constant	Logistic	0.576	0.006	0.571	0.536
500	5000	Decaying MCAR	Linear	Constant	0.163	0.162	0.536	0.536
500	5000	Decaying MCAR	Linear	Logistic	0.163	0.162	0.571	0.536
500	5000	Decaying logistic	Constant	Constant	0.426	0.005	0.443	0.425
500	5000	Decaying logistic	Constant	Logistic	1.160	0.005	1.024	0.425
500	5000	Decaying logistic	Linear	Constant	0.162	0.162	0.443	0.425
500	5000	Decaying logistic	Linear	Logistic	0.166	0.162	1.024	0.425
500	50000	Decaying MCAR	Constant	Constant	0.542	0.002	0.541	0.541
500	50000	Decaying MCAR	Constant	Logistic	0.585	0.002	0.579	0.541
500	50000	Decaying MCAR	Linear	Constant	0.057	0.054	0.541	0.541
500	50000	Decaying MCAR	Linear	Logistic	0.057	0.054	0.579	0.541
500	50000	Decaying logistic	Constant	Constant	0.348	0.001	0.373	0.348
500	50000	Decaying logistic	Constant	Logistic	1.073	0.001	0.912	0.348
500	50000	Decaying logistic	Linear	Constant	0.055	0.054	0.373	0.348
500	50000	Decaying logistic	Linear	Logistic	0.062	0.054	0.912	0.348
1000	10000	Decaying MCAR	Constant	Constant	0.379	0.003	0.379	0.379
1000	10000	Decaying MCAR	Constant	Logistic	0.393	0.003	0.391	0.379
1000	10000	Decaying MCAR	Linear	Constant	0.115	0.114	0.379	0.379
1000	10000	Decaying MCAR	Linear	Logistic	0.115	0.114	0.391	0.379
1000	10000	Decaying logistic	Constant	Constant	0.300	0.002	0.313	0.300
1000	10000	Decaying logistic	Constant	Logistic	0.772	0.002	0.684	0.300
1000	10000	Decaying logistic	Linear	Constant	0.115	0.114	0.313	0.300
1000	10000	Decaying logistic	Linear	Logistic	0.116	0.114	0.684	0.300
1000	100000	Decaying MCAR	Constant	Constant	0.383	0.001	0.382	0.382
1000	100000	Decaying MCAR	Constant	Logistic	0.398	0.001	0.396	0.382
1000	100000	Decaying MCAR	Linear	Constant	0.040	0.038	0.382	0.382
1000	100000	Decaying MCAR	Linear	Logistic	0.040	0.038	0.396	0.382
1000	100000	Decaying logistic	Constant	Constant	0.246	0.001	0.264	0.246
1000	100000	Decaying logistic	Constant	Logistic	0.756	0.001	0.643	0.246
1000	100000	Decaying logistic	Linear	Constant	0.039	0.038	0.264	0.246
1000	100000	Decaying logistic	Linear	Logistic	0.043	0.038	0.643	0.246

Table C.3: Multivariate outcome mean simulation results. Average width of component-wise confidence intervals is reported for four different estimators. Each row corresponds to a specific configuration of labeled and unlabeled sample sizes, with $n \in \{100, 500, 1000\}$ and $N \in \{10n, 100n\}$, setting, and models for the nuisance functions.

n	N	Setting	μ model	π model	AIPW	OR	IPW	Naive
100	1000	Decaying MCAR	Constant	Constant	0.932	0.495	0.940	0.934
100	1000	Decaying MCAR	Constant	Logistic	1.000	0.495	1.000	0.934
100	1000	Decaying MCAR	Linear	Constant	0.956	0.953	0.940	0.934
100	1000	Decaying MCAR	Linear	Logistic	0.950	0.953	1.000	0.934
100	1000	Decaying logistic	Constant	Constant	0.139	0.486	0.141	0.211
100	1000	Decaying logistic	Constant	Logistic	0.970	0.486	0.963	0.211
100	1000	Decaying logistic	Linear	Constant	0.947	0.950	0.141	0.211
100	1000	Decaying logistic	Linear	Logistic	0.945	0.950	0.963	0.211
100	10000	Decaying MCAR	Constant	Constant	0.945	0.486	0.949	0.948
100	10000	Decaying MCAR	Constant	Logistic	1.000	0.486	1.000	0.948
100	10000	Decaying MCAR	Linear	Constant	0.956	0.924	0.949	0.948
100	10000	Decaying MCAR	Linear	Logistic	0.942	0.924	1.000	0.948
100	10000	Decaying logistic	Constant	Constant	0.065	0.478	0.066	0.134
100	10000	Decaying logistic	Constant	Logistic	0.951	0.478	0.947	0.134
100	10000	Decaying logistic	Linear	Constant	0.940	0.928	0.066	0.134
100	10000	Decaying logistic	Linear	Logistic	0.950	0.928	0.947	0.134
500	5000	Decaying MCAR	Constant	Constant	0.940	0.459	0.940	0.941
500	5000	Decaying MCAR	Constant	Logistic	1.000	0.459	1.000	0.941
500	5000	Decaying MCAR	Linear	Constant	0.957	0.955	0.940	0.941
500	5000	Decaying MCAR	Linear	Logistic	0.958	0.955	1.000	0.941
500	5000	Decaying logistic	Constant	Constant	0.030	0.515	0.030	0.047
500	5000	Decaying logistic	Constant	Logistic	0.977	0.515	0.970	0.047
500	5000	Decaying logistic	Linear	Constant	0.958	0.956	0.030	0.047
500	5000	Decaying logistic	Linear	Logistic	0.961	0.956	0.970	0.047
500	50000	Decaying MCAR	Constant	Constant	0.955	0.471	0.956	0.948
500	50000	Decaying MCAR	Constant	Logistic	1.000	0.471	1.000	0.948
500	50000	Decaying MCAR	Linear	Constant	0.933	0.895	0.956	0.948
500	50000	Decaying MCAR	Linear	Logistic	0.937	0.895	1.000	0.948
500	50000	Decaying logistic	Constant	Constant	0.008	0.511	0.008	0.025
500	50000	Decaying logistic	Constant	Logistic	0.956	0.511	0.950	0.025
500	50000	Decaying logistic	Linear	Constant	0.923	0.912	0.008	0.025
500	50000	Decaying logistic	Linear	Logistic	0.938	0.912	0.950	0.025
1000	10000	Decaying MCAR	Constant	Constant	0.943	0.505	0.945	0.945
1000	10000	Decaying MCAR	Constant	Logistic	1.000	0.505	1.000	0.945
1000	10000	Decaying MCAR	Linear	Constant	0.959	0.959	0.945	0.945
1000	10000	Decaying MCAR	Linear	Logistic	0.961	0.959	1.000	0.945
1000	10000	Decaying logistic	Constant	Constant	0.013	0.498	0.013	0.021
1000	10000	Decaying logistic	Constant	Logistic	0.974	0.498	0.970	0.021
1000	10000	Decaying logistic	Linear	Constant	0.959	0.958	0.013	0.021
1000	10000	Decaying logistic	Linear	Logistic	0.959	0.958	0.970	0.021
1000	100000	Decaying MCAR	Constant	Constant	0.965	0.503	0.965	0.960
1000	100000	Decaying MCAR	Constant	Logistic	1.000	0.503	1.000	0.960
1000	100000	Decaying MCAR	Linear	Constant	0.956	0.924	0.965	0.960
1000	100000	Decaying MCAR	Linear	Logistic	0.958	0.924	1.000	0.960
1000	100000	Decaying logistic	Constant	Constant	0.007	0.490	0.007	0.014
1000	100000	Decaying logistic	Constant	Logistic	0.957	0.490	0.963	0.014
1000	100000	Decaying logistic	Linear	Constant	0.934	0.921	0.007	0.014
1000	100000	Decaying logistic	Linear	Logistic	0.952	0.921	0.963	0.014

Table C.4: Multivariate outcome mean simulation results. Joint empirical coverage is reported for four different estimators. Each row corresponds to a specific configuration of labeled and unlabeled sample sizes, with $n \in \{100, 500, 1000\}$ and $N \in \{10n, 100n\}$, setting, and models for the nuisance functions.

n	N	Setting	μ model	π model	AIPW	OR	IPW	Naive
100	1000	Decaying MCAR	Constant	Constant	0.300	0.974	0.297	0.010
100	1000	Decaying MCAR	Constant	Logistic	0.549	0.974	0.509	0.010
100	1000	Decaying MCAR	Linear	Constant	0.011	0.012	0.297	0.010
100	1000	Decaying MCAR	Linear	Logistic	0.015	0.012	0.509	0.010
100	1000	Decaying logistic	Constant	Constant	0.244	0.974	0.315	0.008
100	1000	Decaying logistic	Constant	Logistic	0.975	0.974	0.850	0.008
100	1000	Decaying logistic	Linear	Constant	0.009	0.009	0.315	0.008
100	1000	Decaying logistic	Linear	Logistic	0.026	0.009	0.850	0.008
100	10000	Decaying MCAR	Constant	Constant	0.313	0.976	0.310	0.010
100	10000	Decaying MCAR	Constant	Logistic	0.554	0.976	0.515	0.010
100	10000	Decaying MCAR	Linear	Constant	0.011	0.011	0.310	0.010
100	10000	Decaying MCAR	Linear	Logistic	0.015	0.011	0.515	0.010
100	10000	Decaying logistic	Constant	Constant	0.204	0.976	0.462	0.006
100	10000	Decaying logistic	Constant	Logistic	0.720	0.976	0.611	0.006
100	10000	Decaying logistic	Linear	Constant	0.007	0.007	0.462	0.006
100	10000	Decaying logistic	Linear	Logistic	0.019	0.007	0.611	0.006
500	5000	Decaying MCAR	Constant	Constant	0.134	0.969	0.134	0.004
500	5000	Decaying MCAR	Constant	Logistic	0.154	0.969	0.150	0.004
500	5000	Decaying MCAR	Linear	Constant	0.004	0.005	0.134	0.004
500	5000	Decaying MCAR	Linear	Logistic	0.005	0.005	0.150	0.004
500	5000	Decaying logistic	Constant	Constant	0.127	0.969	0.219	0.003
500	5000	Decaying logistic	Constant	Logistic	0.305	0.969	0.274	0.003
500	5000	Decaying logistic	Linear	Constant	0.004	0.004	0.219	0.003
500	5000	Decaying logistic	Linear	Logistic	0.008	0.004	0.274	0.003
500	50000	Decaying MCAR	Constant	Constant	0.139	0.972	0.139	0.004
500	50000	Decaying MCAR	Constant	Logistic	0.160	0.972	0.156	0.004
500	50000	Decaying MCAR	Linear	Constant	0.004	0.004	0.139	0.004
500	50000	Decaying MCAR	Linear	Logistic	0.005	0.004	0.156	0.004
500	50000	Decaying logistic	Constant	Constant	0.096	0.972	0.410	0.003
500	50000	Decaying logistic	Constant	Logistic	0.300	0.972	0.257	0.003
500	50000	Decaying logistic	Linear	Constant	0.003	0.003	0.410	0.003
500	50000	Decaying logistic	Linear	Logistic	0.008	0.003	0.257	0.003
1000	10000	Decaying MCAR	Constant	Constant	0.094	0.963	0.094	0.003
1000	10000	Decaying MCAR	Constant	Logistic	0.100	0.963	0.099	0.003
1000	10000	Decaying MCAR	Linear	Constant	0.003	0.003	0.094	0.003
1000	10000	Decaying MCAR	Linear	Logistic	0.003	0.003	0.099	0.003
1000	10000	Decaying logistic	Constant	Constant	0.100	0.963	0.198	0.002
1000	10000	Decaying logistic	Constant	Logistic	0.206	0.963	0.184	0.002
1000	10000	Decaying logistic	Linear	Constant	0.003	0.003	0.198	0.002
1000	10000	Decaying logistic	Linear	Logistic	0.006	0.003	0.184	0.002
1000	100000	Decaying MCAR	Constant	Constant	0.098	0.969	0.098	0.003
1000	100000	Decaying MCAR	Constant	Logistic	0.105	0.969	0.104	0.003
1000	100000	Decaying MCAR	Linear	Constant	0.003	0.003	0.098	0.003
1000	100000	Decaying MCAR	Linear	Logistic	0.003	0.003	0.104	0.003
1000	100000	Decaying logistic	Constant	Constant	0.072	0.969	0.379	0.002
1000	100000	Decaying logistic	Constant	Logistic	0.222	0.969	0.192	0.002
1000	100000	Decaying logistic	Linear	Constant	0.002	0.002	0.379	0.002
1000	100000	Decaying logistic	Linear	Logistic	0.006	0.002	0.192	0.002

Table C.5: Linear regression coefficients simulation results. RMSE is reported for four different estimators. Each row corresponds to a specific configuration of labeled and unlabeled sample sizes, with $n \in \{100, 500, 1000\}$ and $N \in \{10n, 100n\}$, setting, and models for the nuisance functions.

n	N	Setting	μ model	π model	AIPW	OR	IPW	Naive
100	1000	Decaying MCAR	Constant	Constant	0.954	0.017	0.954	0.920
100	1000	Decaying MCAR	Constant	Logistic	0.942	0.017	0.950	0.920
100	1000	Decaying MCAR	Linear	Constant	0.934	0.162	0.954	0.920
100	1000	Decaying MCAR	Linear	Logistic	0.959	0.162	0.950	0.920
100	1000	Decaying logistic	Constant	Constant	0.952	0.039	0.899	0.932
100	1000	Decaying logistic	Constant	Logistic	0.950	0.039	0.956	0.932
100	1000	Decaying logistic	Linear	Constant	0.942	0.172	0.899	0.932
100	1000	Decaying logistic	Linear	Logistic	0.948	0.172	0.956	0.932
100	10000	Decaying MCAR	Constant	Constant	0.951	0.006	0.952	0.928
100	10000	Decaying MCAR	Constant	Logistic	0.947	0.006	0.954	0.928
100	10000	Decaying MCAR	Linear	Constant	0.941	0.057	0.952	0.928
100	10000	Decaying MCAR	Linear	Logistic	0.961	0.057	0.954	0.928
100	10000	Decaying logistic	Constant	Constant	0.961	0.017	0.835	0.944
100	10000	Decaying logistic	Constant	Logistic	0.939	0.017	0.945	0.944
100	10000	Decaying logistic	Linear	Constant	0.955	0.062	0.835	0.944
100	10000	Decaying logistic	Linear	Logistic	0.950	0.062	0.945	0.944
500	5000	Decaying MCAR	Constant	Constant	0.956	0.004	0.956	0.946
500	5000	Decaying MCAR	Constant	Logistic	0.950	0.004	0.953	0.946
500	5000	Decaying MCAR	Linear	Constant	0.950	0.079	0.956	0.946
500	5000	Decaying MCAR	Linear	Logistic	0.956	0.079	0.953	0.946
500	5000	Decaying logistic	Constant	Constant	0.917	0.017	0.833	0.944
500	5000	Decaying logistic	Constant	Logistic	0.951	0.017	0.950	0.944
500	5000	Decaying logistic	Linear	Constant	0.948	0.089	0.833	0.944
500	5000	Decaying logistic	Linear	Logistic	0.949	0.089	0.950	0.944
500	50000	Decaying MCAR	Constant	Constant	0.955	0.002	0.955	0.946
500	50000	Decaying MCAR	Constant	Logistic	0.951	0.002	0.953	0.946
500	50000	Decaying MCAR	Linear	Constant	0.948	0.024	0.955	0.946
500	50000	Decaying MCAR	Linear	Logistic	0.955	0.024	0.953	0.946
500	50000	Decaying logistic	Constant	Constant	0.956	0.007	0.798	0.951
500	50000	Decaying logistic	Constant	Logistic	0.943	0.007	0.944	0.951
500	50000	Decaying logistic	Linear	Constant	0.959	0.028	0.798	0.951
500	50000	Decaying logistic	Linear	Logistic	0.950	0.028	0.944	0.951
1000	10000	Decaying MCAR	Constant	Constant	0.957	0.002	0.957	0.946
1000	10000	Decaying MCAR	Constant	Logistic	0.955	0.002	0.956	0.946
1000	10000	Decaying MCAR	Linear	Constant	0.947	0.054	0.957	0.946
1000	10000	Decaying MCAR	Linear	Logistic	0.952	0.054	0.956	0.946
1000	10000	Decaying logistic	Constant	Constant	0.889	0.011	0.817	0.947
1000	10000	Decaying logistic	Constant	Logistic	0.947	0.011	0.946	0.947
1000	10000	Decaying logistic	Linear	Constant	0.950	0.056	0.817	0.947
1000	10000	Decaying logistic	Linear	Logistic	0.953	0.056	0.946	0.947
1000	100000	Decaying MCAR	Constant	Constant	0.957	0.001	0.958	0.953
1000	100000	Decaying MCAR	Constant	Logistic	0.956	0.001	0.957	0.953
1000	100000	Decaying MCAR	Linear	Constant	0.952	0.018	0.958	0.953
1000	100000	Decaying MCAR	Linear	Logistic	0.954	0.018	0.957	0.953
1000	100000	Decaying logistic	Constant	Constant	0.944	0.004	0.790	0.950
1000	100000	Decaying logistic	Constant	Logistic	0.946	0.004	0.947	0.950
1000	100000	Decaying logistic	Linear	Constant	0.958	0.021	0.790	0.950
1000	100000	Decaying logistic	Linear	Logistic	0.955	0.021	0.947	0.950

Table C.6: Linear regression coefficients simulation results. Component-wise empirical coverage is reported for four different estimators. Each row corresponds to a specific configuration of labeled and unlabeled sample sizes, with $n \in \{100, 500, 1000\}$ and $N \in \{10n, 100n\}$, setting, and models for the nuisance functions.

n	N	Setting	μ model	π model	AIPW	OR	IPW	Naive
100	1000	Decaying MCAR	Constant	Constant	1.247	0.046	1.237	0.039
100	1000	Decaying MCAR	Constant	Logistic	1.879	0.046	1.803	0.039
100	1000	Decaying MCAR	Linear	Constant	0.045	0.005	1.237	0.039
100	1000	Decaying MCAR	Linear	Logistic	0.063	0.005	1.803	0.039
100	1000	Decaying logistic	Constant	Constant	0.991	0.101	1.014	0.030
100	1000	Decaying logistic	Constant	Logistic	3.450	0.101	3.016	0.030
100	1000	Decaying logistic	Linear	Constant	0.035	0.004	1.014	0.030
100	1000	Decaying logistic	Linear	Logistic	0.095	0.004	3.016	0.030
100	10000	Decaying MCAR	Constant	Constant	1.305	0.015	1.296	0.039
100	10000	Decaying MCAR	Constant	Logistic	1.950	0.015	1.872	0.039
100	10000	Decaying MCAR	Linear	Constant	0.045	0.002	1.296	0.039
100	10000	Decaying MCAR	Linear	Logistic	0.065	0.002	1.872	0.039
100	10000	Decaying logistic	Constant	Constant	0.884	0.042	0.946	0.024
100	10000	Decaying logistic	Constant	Logistic	2.653	0.042	2.275	0.024
100	10000	Decaying logistic	Linear	Constant	0.028	0.001	0.946	0.024
100	10000	Decaying logistic	Linear	Logistic	0.069	0.001	2.275	0.024
500	5000	Decaying MCAR	Constant	Constant	0.558	0.009	0.558	0.017
500	5000	Decaying MCAR	Constant	Logistic	0.604	0.009	0.599	0.017
500	5000	Decaying MCAR	Linear	Constant	0.018	0.001	0.558	0.017
500	5000	Decaying MCAR	Linear	Logistic	0.019	0.001	0.599	0.017
500	5000	Decaying logistic	Constant	Constant	0.444	0.042	0.457	0.014
500	5000	Decaying logistic	Constant	Logistic	1.168	0.042	1.043	0.014
500	5000	Decaying logistic	Linear	Constant	0.015	0.001	0.457	0.014
500	5000	Decaying logistic	Linear	Logistic	0.032	0.001	1.043	0.014
500	50000	Decaying MCAR	Constant	Constant	0.584	0.003	0.583	0.018
500	50000	Decaying MCAR	Constant	Logistic	0.634	0.003	0.628	0.018
500	50000	Decaying MCAR	Linear	Constant	0.018	0.000	0.583	0.018
500	50000	Decaying MCAR	Linear	Logistic	0.019	0.000	0.628	0.018
500	50000	Decaying logistic	Constant	Constant	0.394	0.018	0.424	0.011
500	50000	Decaying logistic	Constant	Logistic	1.156	0.018	0.989	0.011
500	50000	Decaying logistic	Linear	Constant	0.012	0.000	0.424	0.011
500	50000	Decaying logistic	Linear	Logistic	0.029	0.000	0.989	0.011
1000	10000	Decaying MCAR	Constant	Constant	0.393	0.005	0.393	0.012
1000	10000	Decaying MCAR	Constant	Logistic	0.409	0.005	0.407	0.012
1000	10000	Decaying MCAR	Linear	Constant	0.013	0.000	0.393	0.012
1000	10000	Decaying MCAR	Linear	Logistic	0.013	0.000	0.407	0.012
1000	10000	Decaying logistic	Constant	Constant	0.311	0.029	0.321	0.010
1000	10000	Decaying logistic	Constant	Logistic	0.800	0.029	0.712	0.010
1000	10000	Decaying logistic	Linear	Constant	0.010	0.000	0.321	0.010
1000	10000	Decaying logistic	Linear	Logistic	0.021	0.000	0.712	0.010
1000	100000	Decaying MCAR	Constant	Constant	0.412	0.001	0.411	0.012
1000	100000	Decaying MCAR	Constant	Logistic	0.429	0.001	0.427	0.012
1000	100000	Decaying MCAR	Linear	Constant	0.013	0.000	0.411	0.012
1000	100000	Decaying MCAR	Linear	Logistic	0.013	0.000	0.427	0.012
1000	100000	Decaying logistic	Constant	Constant	0.278	0.012	0.297	0.008
1000	100000	Decaying logistic	Constant	Logistic	0.864	0.012	0.745	0.008
1000	100000	Decaying logistic	Linear	Constant	0.009	0.000	0.297	0.008
1000	100000	Decaying logistic	Linear	Logistic	0.021	0.000	0.745	0.008

Table C.7: Linear regression coefficients simulation results. Average width of component-wise confidence intervals is reported for four different estimators. Each row corresponds to a specific configuration of labeled and unlabeled sample sizes, with $n \in \{100, 500, 1000\}$ and $N \in \{10n, 100n\}$, setting, and models for the nuisance functions.

n	N	Setting	μ model	π model	AIPW	OR	IPW	Naive
100	1000	Decaying MCAR	Constant	Constant	0.828	0.000	0.827	0.853
100	1000	Decaying MCAR	Constant	Logistic	0.910	0.000	0.910	0.853
100	1000	Decaying MCAR	Linear	Constant	0.736	0.000	0.827	0.853
100	1000	Decaying MCAR	Linear	Logistic	0.835	0.000	0.910	0.853
100	1000	Decaying logistic	Constant	Constant	0.864	0.000	0.680	0.993
100	1000	Decaying logistic	Constant	Logistic	0.521	0.000	0.600	0.993
100	1000	Decaying logistic	Linear	Constant	0.817	0.000	0.680	0.993
100	1000	Decaying logistic	Linear	Logistic	0.722	0.000	0.600	0.993
100	10000	Decaying MCAR	Constant	Constant	0.762	0.000	0.758	0.849
100	10000	Decaying MCAR	Constant	Logistic	0.864	0.000	0.876	0.849
100	10000	Decaying MCAR	Linear	Constant	0.743	0.000	0.758	0.849
100	10000	Decaying MCAR	Linear	Logistic	0.847	0.000	0.876	0.849
100	10000	Decaying logistic	Constant	Constant	0.902	0.000	0.404	1.000
100	10000	Decaying logistic	Constant	Logistic	0.350	0.000	0.450	1.000
100	10000	Decaying logistic	Linear	Constant	0.880	0.000	0.404	1.000
100	10000	Decaying logistic	Linear	Logistic	0.717	0.000	0.450	1.000
500	5000	Decaying MCAR	Constant	Constant	0.934	0.000	0.934	0.936
500	5000	Decaying MCAR	Constant	Logistic	0.942	0.000	0.946	0.936
500	5000	Decaying MCAR	Linear	Constant	0.931	0.000	0.934	0.936
500	5000	Decaying MCAR	Linear	Logistic	0.941	0.000	0.946	0.936
500	5000	Decaying logistic	Constant	Constant	0.797	0.000	0.372	0.997
500	5000	Decaying logistic	Constant	Logistic	0.612	0.000	0.664	0.997
500	5000	Decaying logistic	Linear	Constant	0.922	0.000	0.372	0.997
500	5000	Decaying logistic	Linear	Logistic	0.866	0.000	0.664	0.997
500	50000	Decaying MCAR	Constant	Constant	0.907	0.000	0.901	0.926
500	50000	Decaying MCAR	Constant	Logistic	0.939	0.000	0.939	0.926
500	50000	Decaying MCAR	Linear	Constant	0.912	0.000	0.901	0.926
500	50000	Decaying MCAR	Linear	Logistic	0.926	0.000	0.939	0.926
500	50000	Decaying logistic	Constant	Constant	0.938	0.000	0.194	1.000
500	50000	Decaying logistic	Constant	Logistic	0.580	0.000	0.620	1.000
500	50000	Decaying logistic	Linear	Constant	0.949	0.000	0.194	1.000
500	50000	Decaying logistic	Linear	Logistic	0.894	0.000	0.620	1.000
1000	10000	Decaying MCAR	Constant	Constant	0.941	0.000	0.938	0.922
1000	10000	Decaying MCAR	Constant	Logistic	0.946	0.000	0.948	0.922
1000	10000	Decaying MCAR	Linear	Constant	0.920	0.000	0.938	0.922
1000	10000	Decaying MCAR	Linear	Logistic	0.934	0.000	0.948	0.922
1000	10000	Decaying logistic	Constant	Constant	0.670	0.000	0.294	0.997
1000	10000	Decaying logistic	Constant	Logistic	0.703	0.000	0.735	0.997
1000	10000	Decaying logistic	Linear	Constant	0.939	0.000	0.294	0.997
1000	10000	Decaying logistic	Linear	Logistic	0.931	0.000	0.735	0.997
1000	100000	Decaying MCAR	Constant	Constant	0.943	0.000	0.943	0.949
1000	100000	Decaying MCAR	Constant	Logistic	0.950	0.000	0.953	0.949
1000	100000	Decaying MCAR	Linear	Constant	0.932	0.000	0.943	0.949
1000	100000	Decaying MCAR	Linear	Logistic	0.948	0.000	0.953	0.949
1000	100000	Decaying logistic	Constant	Constant	0.918	0.000	0.139	1.000
1000	100000	Decaying logistic	Constant	Logistic	0.675	0.000	0.694	1.000
1000	100000	Decaying logistic	Linear	Constant	0.946	0.000	0.139	1.000
1000	100000	Decaying logistic	Linear	Logistic	0.948	0.000	0.694	1.000

Table C.8: Linear regression coefficients simulation results. Joint empirical coverage is reported for four different estimators. Each row corresponds to a specific configuration of labeled and unlabeled sample sizes, with $n \in \{100, 500, 1000\}$ and $N \in \{10n, 100n\}$, setting, and models for the nuisance functions. The significant undercoverage in small samples is due to the fact that the parameter we are targeting here is 10-dimensional.

D Further application details

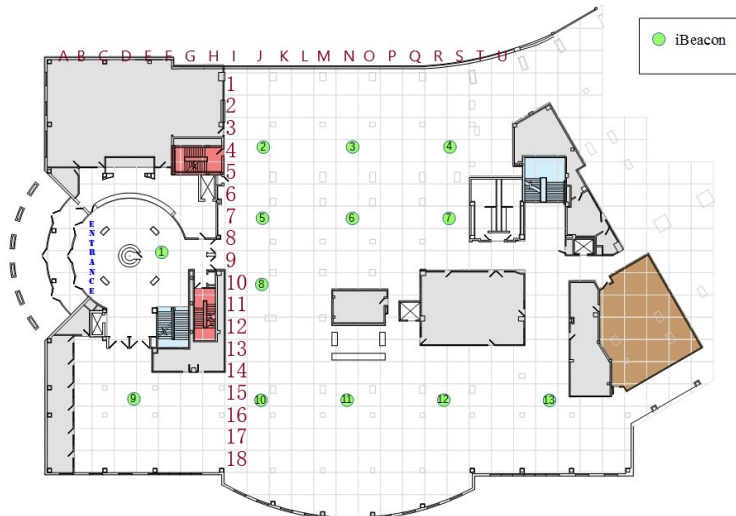


Figure D.2: Layout of library room in BLE-RSSI study. Retrieved from [Mohammadi et al. \(2017\)](#).

D.1 METABRIC study

We further apply our approach to the METABRIC dataset ([Curtis et al., 2012](#); [Pereira et al., 2016](#)), one of the largest open-access breast cancer cohorts with gene expression profiles, clinical covariates, and long-term survival follow-up. [Cheng et al. \(2021\)](#) and [Hsu and Lin \(2023\)](#) identified 20 biomarkers (reported in Supplementary Table D.9) as potentially predictive of 5-year disease-specific survival (DSS) status, and defined two prognosis classes accordingly: the poor prognosis class includes patients who died of breast cancer within five years of diagnosis, while the good prognosis class includes those who died of breast cancer after five years.

Type	Covariates
Biomarkers	ESR1, PGR, ERBB2, MKI67, PLAU, ELAVL1, EGFR, BTRC, FBXO6, SHMT2, KRAS, SRPK2, YWHAQ, PDHA1, EWSR1, ZDHHC17, ENO1, DBN1, PLK1, GSK3B
Clinical features	Age, menopausal state, tumor size, radiotherapy, chemotherapy, hormone therapy, neoplasm histologic grade, cellularity, surgery-breast conserving, surgery-mastectomy

Table D.9: Variables employed in the METABRIC application as described by [Hsu and Lin \(2023\)](#).

Here, we ask a related but complementary question. Instead of discretizing survival outcomes into prognosis classes, we treat survival time (in months) as a continuous response variable. Then, we aim to estimate the effect of the selected biomarkers on survival among patients who died of breast cancer. Following the labeling conventions of [Cheng et al. \(2021\)](#); [Hsu and Lin \(2023\)](#), we treat censored patients – either still alive or deceased from other causes – as unlabeled. The resulting dataset includes $n = 611$ labeled observations and $N = 1231$ unlabeled observations.

We frame this task as a coefficient estimation problem in linear regression. Let Y_i denote the survival time (in months) since initial diagnosis for individual i ; $R_i \in \{0, 1\}$ indicate whether the individual died of breast cancer ($R_i = 1$) or not; $X_i \in \mathbb{R}^p$ represent the vector of expression values for $p = 20$ biomarkers of interest; and $W_i \in \mathbb{R}^s$, with $s = 10$, denote additional clinical features (also described in Supplementary Table D.9) used to aid estimation of nuisance components. The observed data are

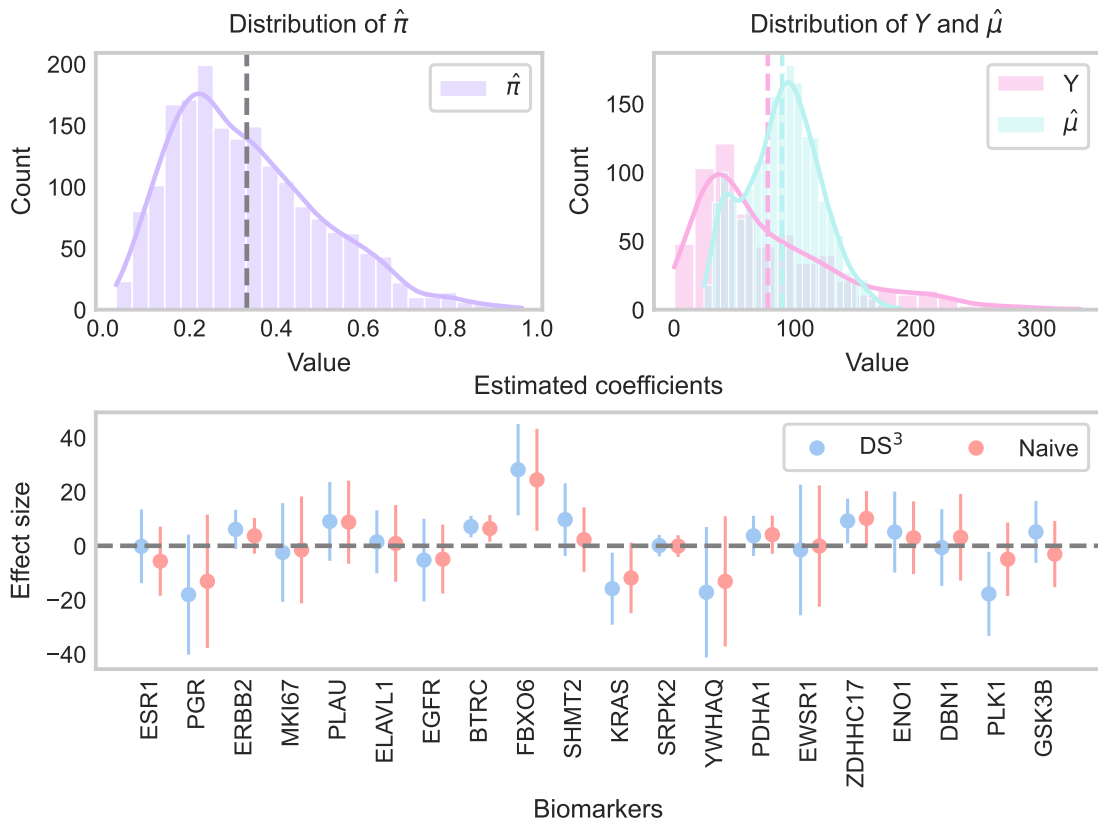


Figure D.3: METABRIC application results. Left panel: estimated propensity scores across observations, along with the proportion of labeled data $n/(n+N)$, shown as a vertical dashed line. The heterogeneity in the estimated propensity scores may suggest a missing-at-random (MAR) labeling mechanism. Right panel: marginal distribution of the observed survival times Y (in months) compared to the distribution of predicted survival times from the estimated outcome model using both biomarkers and clinical covariates. Vertical lines indicate the means of each distribution. The discrepancy between observed and predicted outcomes further suggests a MAR mechanism. Bottom panel: estimated linear coefficients from our semi-supervised approach and the naive estimator based solely on labeled data. Confidence intervals are at $\alpha = 0.1$ significance level.

$\mathcal{D}_i = (X_i, W_i, R_i, R_i Y_i)$, for $i = 1, \dots, n+N$. We employ both the naive estimator, which only analyzes labeled data, and the AIPW estimator in Equation 25. For the latter, the outcome regression model $\hat{\mu}$ is estimated using random forests (Breiman, 2001), with both biomarker and clinical covariates included as predictors. The propensity score $\hat{\pi}$ is estimated via logistic regression, again leveraging both sets of covariates. All nuisance functions are estimated using cross-fitting with $J = 5$ folds to ensure valid inference.

While our approach casts the problem as one of linear regression under distribution shift, we acknowledge that alternative methodological frameworks could also be applied. In particular, since the outcome of interest is survival time, this setting naturally lends itself to tools from survival analysis, such as Cox proportional hazards models (Cox, 1972), which are designed to explicitly account for censoring and time-to-event structure. Moreover, our focus on a fixed, literature-informed set of biomarkers connects to the field of inference after feature selection (Berk et al., 2013; Kuchibhotla et al., 2022), which provides tools for valid inference after variable selection. Although we do not pursue these directions here, our method complements these perspectives by offering a flexible and semiparametrically grounded approach to semi-supervised inference under distribution shift – especially in regimes where labeling is

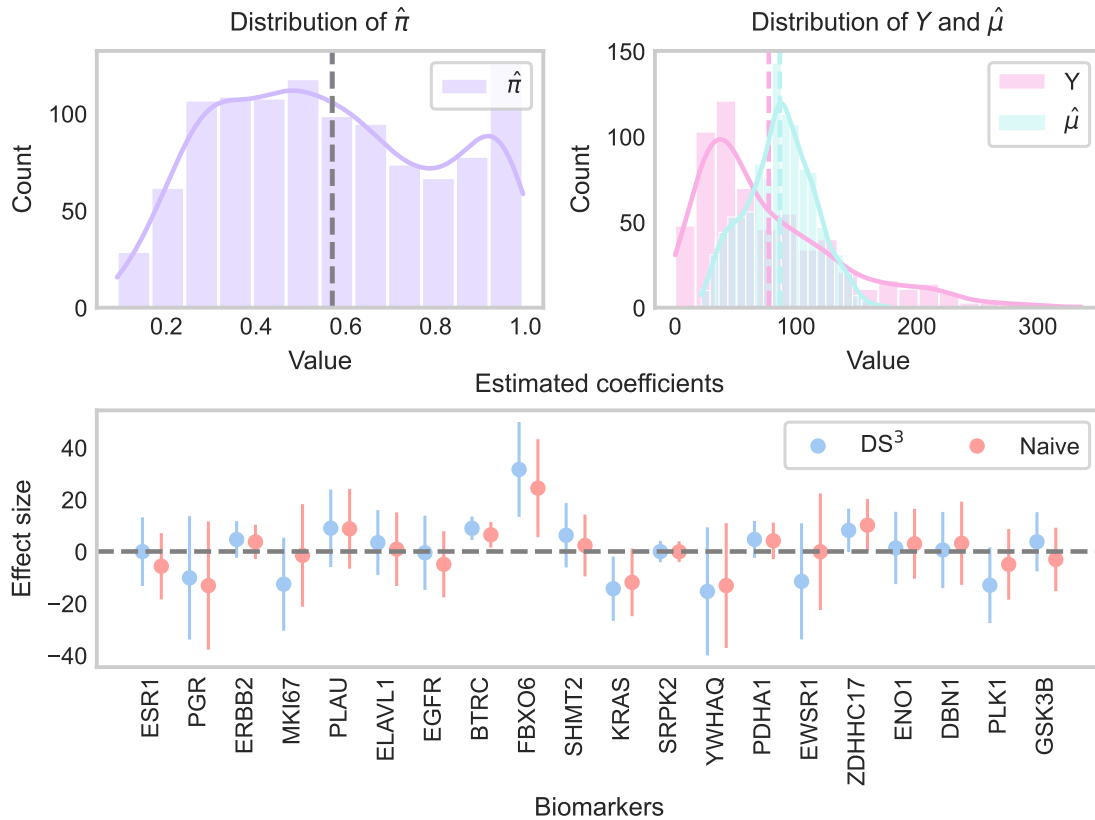


Figure D.4: METABRIC application using only competing risk censored data as unlabeled data.

both biased and sparse.

Results are shown in Supplementary Figure D.3. At the significance level $\alpha = 0.1$, the naive estimator identifies three biomarkers – BTRC, FBXO6, and ZDHHC17 – as significantly associated with survival outcomes. In contrast, our semi-supervised approach identifies two additional significant biomarkers: KRAS and PLK1. Prior studies provide biological support for these findings. Specifically, [Kim et al. \(2015\)](#); [Tokumaru et al. \(2020\)](#) report that elevated KRAS expression is linked to poorer survival outcomes, while [Garlapati et al. \(2023\)](#); [Ueda et al. \(2019\)](#) associate higher PLK1 levels with shorter survival in breast cancer patients.

We note that, because survival times are subject to right-censoring, the missing-at-random (MAR) assumption does not hold: patients with longer survival times are more likely to be censored. However, many patients in METABRIC entered the study at different times, leading to censoring across a range of survival times, not only after five years. Consequently, although the MAR assumption is imperfect, its violation may be moderate in practice. Therefore, to investigate this issue, we repeat our analysis using only those censored observations corresponding to deaths from competing causes, and report results in Supplementary Figure D.4. The results using only competing-risk censored data are qualitatively similar to those obtained using all censored observations, supporting the robustness of our approach despite the potential violation of MAR.

Summarizing, our analysis supports adverse roles for KRAS and PLK1 in breast cancer. These findings underscore the importance of adjusting for distribution shift in semi-supervised survival analyses and demonstrate the practical utility of our proposed approach in real-world biomedical applications.